2015

# Mitochondrial biogenesis and electrical properties of hPSC-derived motor neurons

Laura O'Brien
*Virginia Commonwealth University*, obrienl@vcu.edu

# Mitochondrial biogenesis and electrical properties of hPSC-derived motor neurons

A dissertation submitted in partial fulfillment of the requirements for the degree of Doctor of Philosophy at Virginia Commonwealth University

by

Laura C. O'Brien

Bachelor of Science in Psychology

Kansas State University, 2010

Advisor: James P. Bennett, Jr, MD, PhD

Professor, Neurology, Physiology and Biophysics

Virginia Commonwealth University

Richmond, Virginia

April 2015

## ACKNOWLEDGMENTS

I would like to express my gratitude toward everyone who has helped me along this incredible journey. First I would like to thank my advisor, Dr. Jim Bennett, for allowing me to pursue neuroscience research and for providing lots of 'big picture' advice. I would like to thank all past and present members of the Bennett lab for providing training, advice and feedback. In particular I would like to thank Drs. Amy Ladd and Ann Rice for letting me bounce off ideas and their thoughtful review of countless documents.

My sincerest thanks to my committee members for their advice and constructive criticism. I thank Dr. Diomedes Logothetis for 'adopting' me into his lab and believing in me not only as a scientist but wholly as a person. Thank you for not believing me when I said that I wanted to quit. I would also like to thank Dr. Carlitos Villalba-Galea for the countless hours he spent helping me set up the electrophysiology rig. I thank the staff of the Department of Physiology and Biophysics, especially Christina Kyrus, for being so enthusiastic and supportive.

Finally I would like to thank my family for their unconditional love and support. I especially thank my husband James for encouraging me to follow my dream and for standing by me every step of the way.

## TABLE OF CONTENTS

ACKNOWLEDGMENTS……..ii

LIST OF FIGURES……vii

LIST OF ABBREVIATIONS……..viii

ABSTRACT……...x

CHAPTER ONE: INTRODUCTION……...1

1.1. Mitochondrial biogenesis……...1

1.1.1. Mitobiogenesis signaling……..…2

1.1.2. Mitobiogenesis in ALS……..…5

1.2. Differentiation of motor neurons *in vivo*……6

1.2.1. Signaling during development……....7

1.2.2. Electrical properties of embryonic MN……..…9

1.3. Intrinsic susceptibility of motor neurons……11

1.3.1. Calcium buffering……11

1.3.2. Plateau potentials……...14

1.3.3. Repetitive firing……...14

1.3.4. Properties altered in ALS ……16

1.4. hPSCs……17

1.4.1. Reprogramming of somatic cells……..17

1.4.2. Using iPSCs to study ALS……19

1.4.3. Mitochondrial regulation in hPSCs……..20

1.4.4. Low oxygen conditions……..21

1.5. Aims of the study……..22

2. CHAPTER TWO: GENERAL METHODS……23

2.1. Culture of hESC-derived hNSCs……..23

2.2. iPSC generation and neural induction……..23

2.3. Differentiation of hNSCs into motor neurons……25

2.4. Nucleic acid isolation and cDNA synthesis……..26

2.5. Quantitative PCR……..26

2.6. mtDNA copy number……31

2.7. Confocal microscopy and immunofluorescence…….……31

2.8. Western blot analysis……..32

2.9. XF24 extracellular flux analyzer……..33

2.10. Lentiviral generation and infection……...34

2.11. Electrophysiology……...34

2.12. Statistical analysis……..35

3. CHAPTER THREE…….....36

*Generation of motor neurons from embryonic and iPSC-derived human neural stem cells*

3.1. Rationale and hypothesis……....36

3.2. Statement of contributions……...39

3.3. Results……39

3.3.1. Generation of iPSCs from blood PBMCs……39

3.3.2. Neural induction of iPSCs……42
3.3.3. Spontaneous differentiation of NSCs into neurons, astrocytes, and oligodendrocytes……44
3.3.4. Motor neuron differentiation of hESC-derived cells……..46
3.3.5. Differentiation of motor neurons from iPSC-derived cells……48
3.4. Summary……50

4. CHAPTER FOUR……51
*Mitochondrial biogenesis increases as cells differentiate from neural stem cells into motor neurons*
4.1. Rationale and hypothesis……51
4.2. Results……53
4.2.1. Mitobiogenesis signaling increases with motor neuron differentiation……..53
4.2.2. Mitochondrial encoded genes increase with motor neuron differentiation……..55
4.2.3. Glycolysis decreases as cells differentiate into motor neurons…..57
4.2.4. Electron transport chain proteins, but not mitochondrial mass, increase with differentiation……..62
4.3. Summary……65

5. CHAPTER FIVE……66
*Electrophysiological changes as cells differentiate into motor neurons*

5.1. Rationale and hypothesis……66

5.2. Results……66

5.2.1. Identifying motor neurons in live culture……66

5.2.2. Passive membrane properties of hESC and iPSC-derived cells…67

5.2.3. Voltage gated currents characteristic of excitable cells……69

5.2.4. Action potential firing of stem cell derived motor neurons……...71

5.3. Summary……73

6. CHAPTER SIX: DISCUSSION

6.1. Generation of motor neurons from hNSCs……74

6.2. Mitobiogenesis signaling in hPSC derived motor neurons……76

6.3. Electrical maturation of hPSC-derived motor neurons……79

6.4. Use of hPSC-derived motor neurons for disease modeling……...80

6.5. Summary and conclusions……...81

6.6. Significance and perspectives……82

REFERENCES……83

VITA……..93

## LIST OF FIGURES

Figure 1. Mitobiogenesis signaling……4

Figure 2. Motor neuron specification in the developing embryo……...8

Figure 3. Primer sets used in the present study……28

Figure 4. Schematic of motor neuron differentiation……37

Figure 5. Generation of iPSCs from blood……..……41

Figure 6. Neural induction of iPSCs……43

Figure 7. Neuronal and glial markers after spontaneous differentiation……45

Figure 8. Motor neuron differentiation of hESC-derived hNSCs……47

Figure 9. Motor neuron differentiation of iPSC-derived hNSCs……49

Figure 10. Mitochondrial biogenesis and ATP production……...52

Figure 11. Mitochondrial biogenesis signaling during motor neuron differentiation

…….....54

Figure 12. Mitochondrial encoded gene expression and mtDNA copy number...56

Figure 13. OCR and ECAR values as a function of cell density……59

Figure 14. Bioenergetic profile of hNSCs and motor neurons……60

Figure 15. ECAR in hNSCs and motor neurons……61

Figure 16. Respiratory chain protein expression in hNSCs and motor neurons..63

Figure 17. Mitochondrial mass in hNSCs and motor neurons……64

Figure 18. Passive membrane properties in hNSC-derived motor neurons…….68

Figure 19. Voltage gated currents in hNSC-derived motor neurons……..70

Figure 20. Action potential generation in hNSC-derived motor neurons……...72

## LIST OF ABBREVIATIONS

| | |
|---|---|
| AHP | Afterhyperpolarization |
| ALS | Amyotrophic lateral sclerosis |
| BMP | Bone morophgenic protein |
| ChAT | Choline acetyltransferase |
| Cm | Membrane capacitance |
| ECAR | Extracellular acidification rate |
| ERRα | Estrogen-related receptor α |
| ETC | Electron transport chain |
| fALS | Familial ALS |
| FP | Floor plate |
| FUS | Fused in sarcoma |
| GALC | Galactocerebroside |
| GLT-1 | Glial glutamate transporter-1 |
| GFAP | Glial Fibrillary Acidic Protein |
| hESC | Human embryonic stem cell |
| hNSC | Human neural stem cell |
| hPSC | Human pluripotent stem cell |
| iPSC | Induced pluripotent stem cell |
| ISL1, 2 | Islet 1 and Islet 2 |
| MAP2 | Microtubule-associated protein 2 |
| Mitobiogenesis | Mitochondrial biogenesis |
| mtDNA | Mitochondrial DNA |
| NEFL | Neural filament light chain |
| NRF1 | Nuclear respiratory factor 1 |
| NRF2 | Nuclear respiratory factor 2 |
| NSE | Neuron specific enolase |
| OCR | Oxygen consumption rate |
| OXPHOS | Oxidative phosphorylation |
| PBMC | Peripheral blood mononuclear cell |
| PGC-1α | Peroxisome proliferator-activated receptor gamma, co-activator 1-α |
| PIC | Persistent inward current |
| PM | Purmorphamine |
| POLG | Mitochondrial DNA polymerase gamma |
| POLRMT | Mitochondrial DNA-directed RNA polymerase |
| qPCR | Quantitative real time PCR |
| RA | Retinoic acid |
| ROCK | Rho-associated protein kinase |
| ROS | Reactive Oxygen Species |
| RP | Roof plate |
| sALS | Sporadic ALS |
| SHH | Sonic hedgehog |
| SK channel | Small conductance calcium-activated potassium channel |
| SOD1 | Cu, Zn superoxide dismutase |
| SV40 | Simian virus 40 |

| | |
|---|---|
| TDP43 | TAR DNA-binding protein 43 |
| TFAM | Mitochondrial transcription factor A |
| TFMB2 | Mitochondrial transcription factor B2 |
| TOM20 | Translocase of outer mitochondrial membranes 20 |
| TUBB3 | Beta III tubulin |
| VDAC1 | Voltage-dependent anion channel 1 |

## ABSTRACT

Human pluripotent stem cells (hPSCs), including human embryonic stem cells (hESCs) and induced pluripotent stem cells (iPSCs) hold great promise in the fields of drug development and regenerative medicine. If iPSCs reprogrammed from patient cells replicate what is seen *in vivo* they may be used as a model of disease. A process that is disrupted in many neurodegenerative diseases is mitochondrial biogenesis. One of these diseases is amyotrophic lateral sclerosis (ALS), which is characterized by loss of motor neurons in the brain and spinal cord. Differentiation of hPSCs into motor neurons offers a way to study a previous unavailable cell type and may further our understanding of human motor neuron biology. The aims of the present study were to differentiate motor neurons from hESCs and iPSCs in low oxygen conditions and to explore mitochondrial biogenesis and electrical maturation during this process. After three weeks of treatment with retinoic acid and purmorphamine, a sonic hedgehog agonist, cells increased expression of post mitotic spinal motor neuron markers. One week later electrophysiological analysis revealed voltage-gated currents and action potential generation. Mitochondrial biogenesis signaling and expression of respiratory chain proteins increased with motor neuron differentiation. Respiration analysis revealed a decrease in glycolysis in motor neurons compared to neural stem cells. Interestingly, this was not accompanied by an increase in basal respiration or mitochondrial mass. These findings enhance our understanding of motor neuron mitochondrial biogenesis, a process impaired in ALS.

# CHAPTER ONE: INTRODUCTION

Amyotrophic lateral sclerosis (ALS) is a devastating neurodegenerative disease characterized by loss of motor neurons in the brain and spinal cord. Despite extensive study, the mechanisms underlying the pathogenesis of sporadic ALS (sALS) are currently unknown. Recent studies in our laboratory and others have identified increased mitochondrial DNA (mtDNA) deletions, decreased electron transport chain (ETC) subunits, and decreased mitochondrial biogenesis (mitobiogenesis) signaling in post mortem tissue from sALS patients [1-5]. This bioenergetic impairment may provide evidence as to why motor neurons are specifically vulnerable in this disease. If ALS patient cells are unable to maintain a healthy population of mitochondria this could lead to mitochondrial dysfunction, decreased ATP production, and death of vulnerable cells like motor neurons. In order to study mitobiogenesis in human motor neurons, the current project uses human pluripotent stem cells (hPSCs) from healthy patients. The following chapter will review our current understanding of mitochondrial biogenesis signaling, differentiation of motor neurons *in vivo* and how we can replicate this *in vitro* in order to study the mechanisms underlying motor neuron death in ALS.

## 1.1 Mitochondrial biogenesis

Mitochondria play a role in many vital cell functions including ATP synthesis, calcium homeostasis, reactive oxygen species (ROS) production, and apoptosis. In high energy requiring post-mitotic tissues like brain, skeletal muscle, and heart, mitochondrial dysfunction is particularly damaging because cells cannot rid themselves of defective mitochondria by replicating. These cells rely on mitobiogenesis to produce mitochondrial

components, and mitophagy, fission and fusion as “quality control” mechanisms to maintain a population of functional mitochondria.

### 1.1.1 Mitobiogenesis signaling

Mitochondria are unique organelles in that they have their own genome. The double-stranded, circular mammalian mitochondrial genome encodes 13 proteins that are essential for respiratory chain function and oxidative phosphorylation, 2 rRNAs and 22 tRNAs [6, 7]. Mitochondria are not self-sufficient, however, and rely on the nuclear genome to encode most of the ~1200-1500 proteins they require. Mitochondrial DNA (mtDNA) is particularly susceptible to damage by ROS because it has no histones, it is physically close to the respiratory chain where most ROS are generated, and mitochondria have only limited enzymes for repair of oxidatively damaged DNA. Deletions in mtDNA may arise from aberrant repair of oxidatively damaged mtDNA, have been found in tissues including the brain, skeletal muscle, and heart, and accumulate with age [8]. Low levels of these deletions would not be immediately harmful because cells have thousands of copies of mtDNA. However, with age or disease, mutations and deletions can accumulate [9, 10] and lead to decreased mitochondrial respiration and ATP production. Most mtDNA deletions and mutations are heteroplasmic, meaning the cell has a mixture of normal and mutated mitochondrial DNA, but mutations can be homoplasmic as well [11].

As depicted in **Figure 1**, mitobiogenesis is the process by which cells increase their mitochondrial components, which includes transcription of genes encoded by both the mitochondrial and nuclear genomes. Peroxisome proliferator-activated receptor

gamma, co-activator 1-α (PGC-1α) is an upstream regulator of transcription factors involved in mitobiogenesis and respiration including nuclear respiratory factors 1 and 2 (NRF1, NRF2) and mitochondrial transcription factor A (TFAM) [12, 13]. For this reason PGC-1α is thought to be the 'master regulator' of mitobiogenesis. PGC-1$\alpha$ is regulated by chromatin remodeling [14, 15] as well as posttranslational modification [16]. PCG-1α interacts directly with NRF1 and 2 and estrogen-related receptor α (ERRα) which then translocate to the nucleus [17-19]. This results in an increased transcription of genes including those encoding ETC subunits and TFAM, which are then localized to the mitochondria [20]. TFAM is required for mtDNA maintenance and stimulates its bidirectional transcription [21]. A mitochondrial DNA-directed RNA polymerase (POLRMT) and mitochondrial DNA polymerase gamma (POLG) then perform mtDNA transcription and replication, respectively [22].

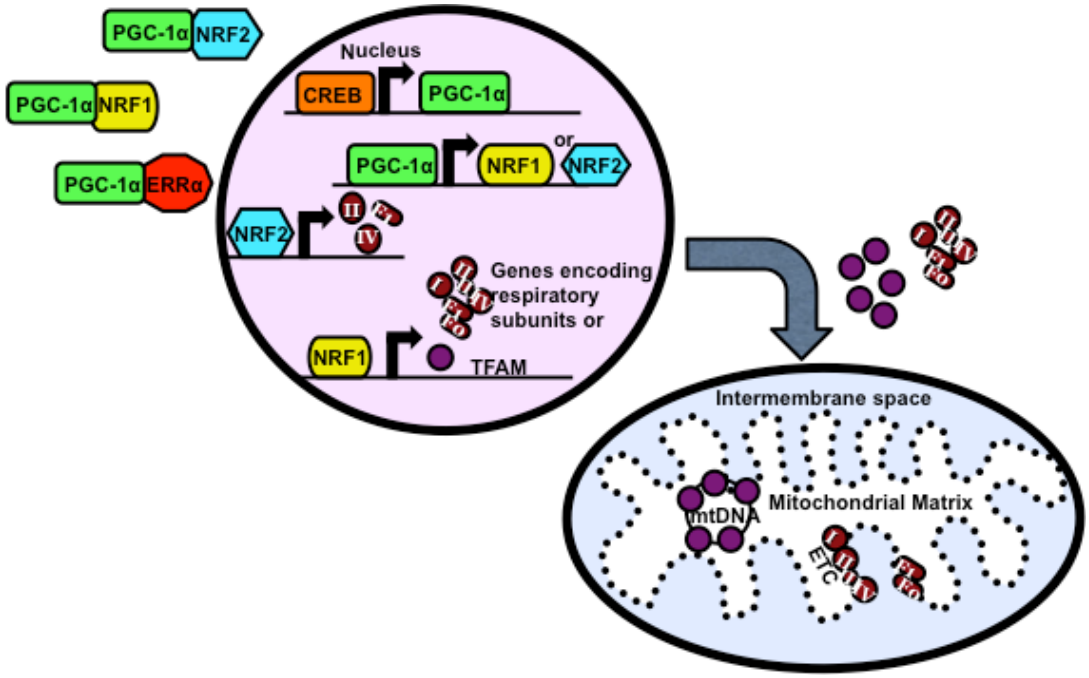


**Figure 1. Mitobiogenesis signaling.** PGC-1α binds to NRF1/2 and ERRα, initiating gene expression of mitochondrial components

### 1.1.2 Mitobiogenesis in ALS

Mitochondrial dysfunction has been well characterized in a number of neurodegenerative diseases including Parkinson's disease, Alzheimer's disease, and ALS. ALS is characterized by loss of both upper motor neurons in the cerebral cortex and lower motor neurons in the brainstem and spinal cord. Death of lower motor neurons leads to progressive muscle weakness and atrophy with respiratory failure being the leading cause of death an average of three to five years after diagnosis [23, 24]. ALS presents in late adulthood, is more common in men than women, and affects 2-5 per 100,000 people worldwide [25]. Over 90% of cases have no family history of the disease, which thus occurs sporadically in most (sALS).

Mitobiogenesis appears to be impaired in post mortem tissues of patients with sALS. PGC-1α and its downstream targets showed decreased expression in post mortem spinal cord and muscle from sALS patients [5]. Additionally, there was decreased activity of ETC subunits and increased mtDNA deletions in isolated post mortem spinal motor neurons [1-3] and skeletal muscle [4] of sALS patients. Mitochondrial encoded gene expression was significantly depressed in peripheral blood mononuclear cells (PBMCs) of sALS patients compared to neurologically healthy controls [26]. This suggests a systemic bioenergetic impairment. Interestingly, healthy human oculomotor neurons isolated from post mortem tissue showed increased gene expression related to mitochondrial function when compared to spinal motor neurons [27]. Upregulation of mitobiogenesis could be a protective mechanism and may be one reason why oculomotor neurons and PBMCs are spared in ALS.

The most widely studied form of ALS is the inherited form of the disease, familial ALS (fALS), which composes only 5-10% of all cases. The first genetic mutation associated with ALS was found in the enzyme Cu, Zn superoxide dismutase 1 (SOD1) and occurs in approximately 20% of fALS patients, less than 2% of total cases. Even less common genetic mutations known to cause ALS are in the RNA-binding proteins TAR DNA-binding protein 43 (TDP43) and fused in sarcoma (FUS), among many others. Recently, hexanucleotide repeats in the non-coding region of the *C9ORF72* gene was found to be responsible for approximately 22% of fALS cases and is present in 4% of sALS cases [28].

A murine model has been created that expresses human mutant SOD1 at supra-physiological levels. This model replicates some components of the disease, however it does not fully mimic the human disease condition. Much of our understanding of the mechanisms of ALS comes from studies using these mice, however translation of drugs and therapies identified by this model into patients has been disappointing. The only FDA approved treatment for ALS is riluzole; however, it was shown to only increase patient survival by two to three months and does not reverse progression of the disease [29].

### 1.2 Differentiation of motor neurons *in vivo*

There are unique signaling cascades during development that define the identity of every type of cell in the body. In order to make motor neurons *in vitro* we need to understand what normally happens during human development *in vivo*.

### 1.2.1 Signaling during development

Spinal motor neurons are some of the most well characterized cell types in terms of their embryonic origin. Early in development the inner cell mass of the blastocyst specifies into the three germ layers: endoderm, ectoderm, and mesoderm. The patterning of the nervous system is due to repressing and activating signals from a multitude of transcription factors and other proteins [30]. This process is summarized in **Figure 2**, adapted from [31]. The dorsal portion of the ectoderm becomes the nervous system through inhibition of bone morphogenic proteins (BMPs) and activin signaling [32, 33]. After formation of the neural tube the hindbrain and spinal cord is specified from the forebrain and midbrain along the rostro-caudal axis by retinoic acid [34] (RA; Figure 2A). Following this, dorsoventral signaling specifies cell types [35] (**Figure 2B**). Motor neurons derive from the ventral portion of the neural tube and receive a high concentration of sonic hedgehog (SHH) signaling from the notochord and floor plate (FP). Opposing SHH is a concentration of BMP/TGFβ signaling from the roof plate. Also during this time RA is continuing to be released from somites [34]. These signaling gradients produce a grid-like order to the 5 progenitor domains of the spinal cord, V0-V3 interneurons and motor neurons (Figure 2B). SHH signaling activates homeodomain domain protein Nkx6.1, which induces transcription of MNR2, among others [30, 36]. MNR2 is a transcription factor is critical to the differentiation of motor neurons [36]. Following its expression cells exit the cell cycle and express Islet 1 and 2 (Isl1, Isl2) and the motor neuron specific transcription factor HB9 [30].

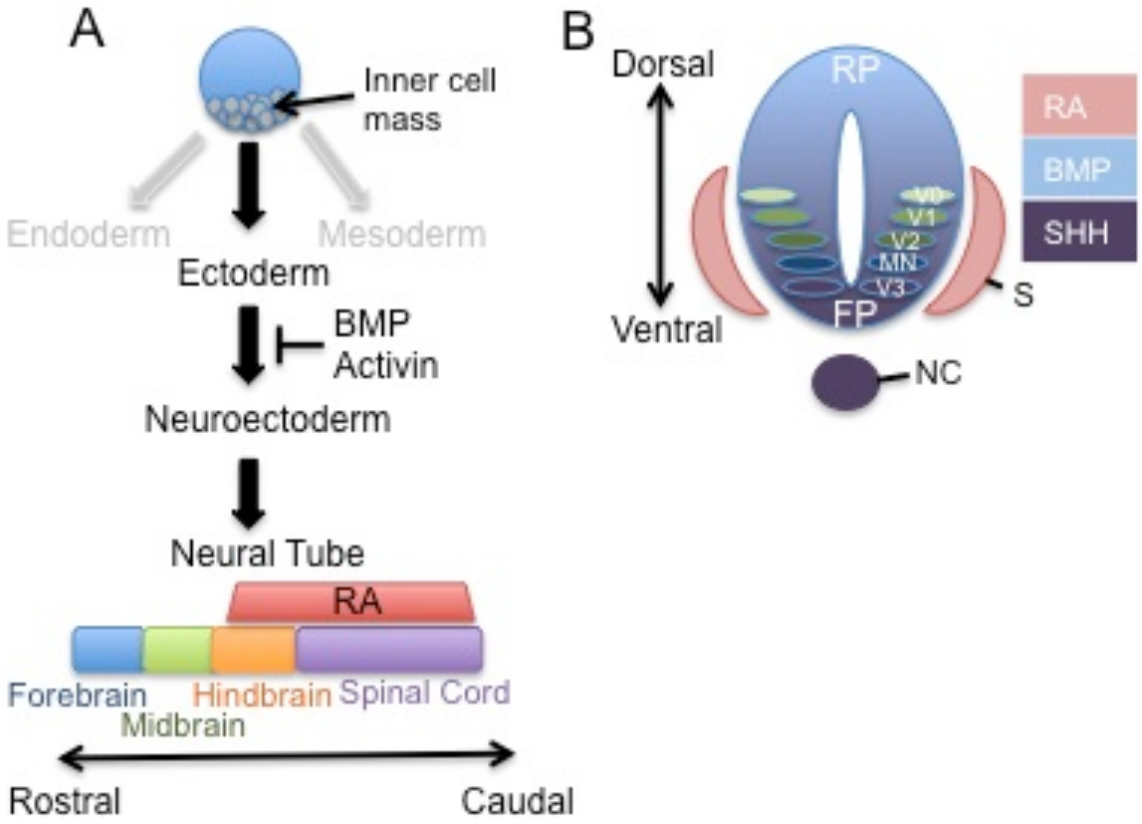


**Figure 2. Motor neuron specification in the developing embryo** A) Motor neurons derive from the dorsal ectoderm in response to inhibition of BMP and activin signaling and retinoic acid B) BMP signaling from the roof plate (RP) opposes sonic hedgehog (SHH) signaling from the notochord (NC) and floor plate (FP). Retinoic acid (RA) is released from the somites (S).

### 1.2.2 Electrical properties of embryonic spinal motor neurons

As motor neurons differentiate there is a dramatic change in passive membrane properties as well as an increase in soma size and neurite complexity. Passive membrane properties including input resistance and membrane time constant decrease during postnatal development of rat motor neurons [37]. Resting membrane potential becomes more hyperpolarized during late embryonic development of rat motor neurons [38] but then remains unchanged from neonatal to adult cells [37]. Membrane capacitance (Cm), an indicator of cell surface area, is increased during embryonic development of rat spinal motor neurons [39]. Many of these findings are replicated in motor neurons differentiated from human embryonic stem cells (hESCs). Input resistance, but not resting membrane potential, decreased [40] and soma size and complexity of neurite outgrowth increased during hESC-derived motor neuron maturation [40].

Voltage-gated ion channels are critical to proper motor neuron function. The major currents that underlie motor neuron resting membrane potential and action potential are sodium, potassium, and calcium currents. These currents are present at a very early stage in development and undergo changes during motor neuron maturation.

All four voltage gated sodium channel subunits expressed in the central nervous system are also expressed in embryonic rat motor neurons, $Na_v1.1$, 1.2, 1.3, and 1.6 [41]. Previous studies in multiple animal models have identified that the upswing of the motor neuron action potential is underlay by the fast inactivating sodium current. The action potential is kept short by the fast inactivation of these channels and the necessity to return to the resting membrane potential before reactivation allows for a refractory

period in which another action potentials cannot be initiated. In this way recovery from inactivation of voltage gated sodium channels can control action potential firing frequency. Detailed activation and inactivation kinetics are difficult to study in motor neurons using voltage-clamp techniques. Due to their large size, the membrane takes more time to charge and extensive dendritic processes make it difficult to control the voltage of the cell (space clamp).

Potassium currents play important roles in motor neuron resting membrane potential, action potential shape, and firing behavior. Both transient ($I_A$) and delayed rectifier ($I_K$) potassium currents are seen in motor neurons *in vivo* [42] as well as in hESC-derived motor neurons [40]. These currents are responsible for the rapid repolarization of the membrane during an action potential. Potassium channels also underlie the afterhyperpolarization (AHP), a period of membrane hyperpolarization that occurs after an action potential is generated. The AHP can be broken down into fast, medium, and slow components. Large conductance (BK) and small conductance (SK) calcium-activated potassium channels underlie the fast and medium components of the AHP, respectively. It is unknown what channels underlie the slow AHP, but previous studies implicate potassium channels in the KCNQ family [43].

In isolated chick motor neurons there were slightly more sodium currents than potassium currents (~70 pA/pF compared to ~60 pA/pF)[44]. From E4-E11 sodium current density increased 60% and correlated with increased action potential amplitude. During this time there was a large increase (16 fold) in $I_A$ and a small (25%) increase in $I_K$. The increase in $I_A$ resulted in a shortening of action potential duration with motor neuron maturation[44]. Calcium currents matured last, with L- and N- type currents

increasing slightly during E4-11 and T-type currents decreasing[45]. Calcium currents were very small compared to sodium currents, and the fact that TTX blocked action potential generation suggests that action potential generation is sodium channel dependent during this time period.

### 1.3 Intrinsic susceptibility of motor neurons

Alpha (α)-motor neurons are selectively vulnerable in ALS, with fast fatigable (FF) motor units degenerating faster than slow (S) motor units [46]. Interestingly, there are two populations of motor neurons that are spared in the disease. Motor neurons in Onuf's nucleus in the sacral section of the spinal cord that control voluntary bladder and rectal sphincters, and oculomotor nuclei in the brainstem that control voluntary eye movements are spared in both sporadic and genetic forms of ALS [27]. It is unknown why only specific cell types, even within the motor neuron population, are lost in this disease. However, by looking at the properties that distinguish these cells from other cell types may give us insights into why they are more vulnerable.

#### 1.3.1 Calcium buffering

Control of motor neuron excitability is vital to optimal development of sustained muscle contractions [47]. Calcium is a second messenger in many signaling cascades and plays an important role in the repetitive firing properties of motor neurons. An increase in calcium depolarizes the cell and makes it more likely to fire action potential(s). However, increased intracellular calcium could lead to greater reliance on mitochondria to buffer calcium and therefore exacerbate mitochondrial damage caused

by normal aging. Combined with a genetic susceptibility to ALS and/or environmental factors this could lead to ALS pathology.

Motor neurons are predicted to have problems handling large amounts of calcium because of their low content of calcium buffering molecules such as calbindin-D2sK and parvalbumin [48], and their large size [49]. For this reason, they rely on intracellular organelles like mitochondria to take up excess calcium. Previous studies using rat and mouse spinal motor neurons *in vitro* revealed an increased reliance on mitochondria to buffer calcium as compared to other neuron types [50, 51]. In brainstem slices from mice mitochondrial dysfunction induced by blocking complex IV of the ETC or uncoupling ATP synthesis resulted in increased intracellular calcium and excitability of motor neurons [52]. Because mitochondria accumulate cytosolic calcium mainly in a membrane potential ($\Delta\psi_M$)-dependent manner through the calcium uniporter, bioenergetic impairments and/or excessive “leak” of protons across a damaged inner membrane are predicted to lower $\Delta\psi_M$ and reduce mitochondrial calcium buffering. Unfortunately, mitochondria show a decline in bioenergetic function with age and disease. Therefore, aging itself may contribute to motor neuron death due to a reduced capacity for calcium buffering leading to calcium-mediated activation of cell death signaling.

Motor neurons also have a large number of calcium permeable glutamate receptors. Glutamate is an excitatory neurotransmitter and an increase in glutamate leads to an influx of sodium and calcium into the cell. One type of ionotrophic glutamate receptors is the α-amino-3-hydroxyl-5-methyl-4-isoxazole-propionate (AMPA) receptor. Normally pre-mRNA for the GluA2 subunit of the AMPA receptor is edited by adenosine

deaminase acting on RNA 2 (ADAR2) at a specific site, converting adenosine to inosine. During translation, this site is read as an arginine (R) instead of a glutamine (Q). AMPA receptors containing the edited GluA2 subunit conduct mainly sodium; however the lack of this subunit or improper editing allows the channel to conduct calcium as well. Human spinal motor neurons contain a large number of calcium permeable AMPA receptors that lack the GluA2 subunit when compared to other neuron types [53, 54]. Additionally, human oculomotor neurons showed increased expression of the GluR2 subunit compared to spinal motor neurons [27]. Additionally, increased glutamate has been found in the cerebral spinal fluid of sALS patients [55]. This may be explained by loss of the glial glutamate transporter EAAT2 in spinal cord and motor cortex of sALS post mortem tissue [56]. EAAT2, predominately expressed in astrocytes, allows for the uptake of excess glutamate in the extracellular space.

Motor neurons are also unique in their expression of voltage gated calcium channels. They express both high-voltage-activated and low-voltage-activated calcium channels that play a role in action potential duration [42]. High-voltage-activated L-type channels, specifically subtype $Ca_v1.3$, have been shown to mediate the persistent inward current (PIC) that underlies plateau potentials in spinal motor neurons [57, 58]. $Ca_v1.3$ channels open at approximately -55 mV, near the resting membrane potential and 20 mV below the other L-type calcium channel expressed in the mammalian nervous system, $Ca_v1.2$ [59]. This allows calcium influx even at rest or with small depolarizations. In mice there is low expression of $Ca_v1.3$ in spinal motor neurons at birth but expression increases as motor neurons mature, reaching adult levels by

postnatal day 18 [57, 60]. The expression of $Ca_V1.3$ channels in human motor neurons has not been studied.

### 1.3.2 Plateau potentials

Another property of motor neurons is the ability to generate plateau potentials. Plateau potentials are characterized by sustained membrane depolarizations after a stimulus has been terminated. Plateau potentials are activated by excitatory synaptic input or membrane depolarization, which then activates PICs of calcium and sodium. PICs act to amplify incoming signals [61-63]. The sodium PIC is activated quickly but quickly inactivates, and plays an important role in initiating action potentials during repetitive firing [61, 62, 64]. The calcium PIC activates slowly but is persistent and increases in amplitude with repeated excitatory stimulation [62, 65].

### 1.3.3 Repetitive firing

Increased intracellular sodium and calcium and/or a decreased potassium results in a cell that is more likely to fire action potentials. The generation of repetitive action potential firing in response to a sustained stimulus is a characteristic of mature motor neurons. Repetitive firing is modulated by the afterhyperpolarization (AHP). AHP is a period of hyperpolarization after an action potential is fired in which the neuron's membrane potential is lower than normal, inhibiting further action potentials. The AHP can be broken down into fast, medium and slow components (fAHP, mAHP, and sAHP). It is unknown exactly which channels underlie the sAHP, but voltage-gated potassium channels in the KCNQ family have been implicated. Large (BK) and small conductance

calcium-activated potassium (SK) channels underlie the fAHP and mAHP, respectively. When these channels are opened by calcium binding, they allow the efflux of potassium, repolarizing the cell. An increase in SK channel conductance would result in fewer action potentials, while a decrease would result in repetitive firing of action potentials. Motor neurons rely heavily on these channels to mediate the proper balance of repetitive firing.

Lengthening the AHP after an action potential is fired, by activating SK channels, may be beneficial to hyperexcitable motor neurons in sALS patients. Additionally, SK channel activation would result in decreased intracellular calcium through negative feedback on NMDA receptors. When glutamate binds NMDA receptors there is no influx of calcium until there is membrane depolarization, relieving a magnesium block of the channel. When this happens, an increase in intracellular calcium activates SK channels, potassium effluxes, and the membrane repolarizes. Riluzole, the only FDA-approved treatment for ALS, decreases the excitable neurotransmitters glutamate and sodium in the synapse [66]. A recent study suggests that riluzole activates SK channels as well [67]. The fact that riluzole has many targets may explain why it is not more effective in treating ALS. If we were able to determine which mechanism(s) of action were most beneficial for motor neuron survival, we may be able to develop improved drugs that have less unintended activity.

Another current that underlies bursts of action potentials is the hyperpolarization-activated current ($I_h$). Channels that underlie $I_h$ are permeable to both sodium and potassium and $I_h$ acts to return the membrane back to resting after being hyperpolarized [37]. $I_h$ increases with postnatal maturation and underlies rebound depolarizations. This

current may play a role in rebound bursts of action potential firing seen after inhibitory synaptic input in both native and hESC-derived motor neurons [40, 42].

### 1.3.4 Properties altered in ALS

Hyperexcitability has been seen in ALS patients [68-70] and in a mouse model of ALS [71, 72]. In mice, hyperexcitability is one of the earliest phenotypes, occurring long before symptom onset, and appears to be due to active rather than passive membrane properties. There was no change in the resting membrane potential, input resistance, action potential duration, amplitude, or threshold, or in afterhyperpolarization between mice carrying a G93A mutation in SOD1 and controls [71, 72]. There was, however, a significant increase in action potential firing frequency and the amount of current necessary to fire an action potential (rheobase) in the mutant mice [71-73]. This increase in excitability could be due to a number of factors, including increased inward and/or decreased outward currents.

In ALS patients there is evidence for an imbalance of sodium and potassium channels [74, 75]. Increased sodium conductance was seen in motor neurons from fALS patients. In contrast, one study found a decrease in the voltage gated potassium channel Kv1.2 was found in the ventral roots of sALS patients but no change in sodium channels [76]. Alteration in sodium and potassium currents is also seen in the SOD1 mouse model. Motor neurons from SOD1 mutant mice show increases in both sodium and calcium PICs and develop mature action potentials faster than their wild-type counterparts [66]. Isolated embryonic motor neurons from SOD1 mutant mice show

increased recovery from fast inactivation of voltage gated sodium channels when compared to mice expressing normal human SOD1 and wild type mice [77]. This could decrease the refractory period after an action potential is fired, leading to an increase in firing rates.

## 1.4 hPSCs

The classification of human pluripotent stem cells (hPSCs) includes both human embryonic stem cells (hESCs) and induced pluripotent stem cells (iPSCs). hESCs are derived from the inner cell mass of a pre-implantation blastocyst [78]. These cells can divide indefinitely while remaining pluripotent, or can be differentiated into any cell type in the body. Initially there was much hope for hESCs in disease modeling and cell replacement therapies. However, ethical issues and transplantation rejection concerns have limited their use in humans. iPSCs, on the other hand, could be derived from the patients' own cells and therefore have the same genetic background. This would be particularly important for modeling complex diseases like ALS in which there is no one gene mutation that causes the disease. If motor neurons derived from ALS patient iPSCs replicate features seen in the disease they may be useful for understanding ALS pathology and testing therapies.

### 1.4.1 Reprogramming of somatic cells

Initial reprogramming studies found that somatic cells could be reprogrammed into pluripotent cells by nuclear transfer into oocytes [79] or by fusion with ESCs [80, 81]. This suggests that there are soluble factors that determine pluripotency. In 2006

retroviral transduction of four transcription factors, Oct3/4, Sox2, c-Myc, and Klf4, was sufficient to induce reprogramming of mouse fibroblasts [82]. The next year the same was found for human fibroblasts [83]. Since then other cells have been reprogrammed including blood cells [84, 85].

Although integration of foreign DNA is efficient at reprogramming somatic cells, these types of cells would not be safe for clinical use because of their potential for DNA mutations. To address this issue many protocols have been developed to deliver recombinant proteins or mRNA. However, the efficiency of reprogramming using these methods is extremely low and the proteins must be delivered multiple times for a period of several weeks. Another option is to express the reprogramming factors using a non-integrating plasmid. The latent origin of plasmid replication (oriP) and one viral protein, Epstein-Barr Nuclear Antigen 1 (EBNA1) from the Epstein-Barr virus has been shown to be sufficient for replication of the viral plasmid [86] and adding these elements to a plasmid containing four reprogramming factors allows their expression without DNA integration. Expression of the Simian virus 40 (SV40) large T antigen allows for enhanced reprogramming efficiency and the foreign DNA is spontaneously lost after 10-12 passages [87-89]. It is unknown exactly how expression of the SV40 T antigen increases reprogramming efficiency, however it may act to increase transcription replication of the plasmid. This plasmid system has been used to reprogram human peripheral blood mononuclear cells (PBMCs) with a single transfection in as little as 14 days and the epigenetic profile of iPSCs derived from PBMCs shows promoter DNA methylation status more similar to human ES cells than iPSCs derived from fibroblasts [89]. In 2012 a protocol was described that increases the efficiency of PBMC

reprogramming with an improved EBNA1/OriP-based plasmid expressing five reprogramming factors (Oct4, Sox2, Klf4, c-Myc, and Lin28) as a single unit separated by 2A peptide sequences which allows for the co-translational cleavage into individual peptides [90]. PBMCs isolated from as little as five milliliters of peripheral blood can be used fresh or after freezing and lymphocytes are eliminated before reprogramming to reduce the chance of somatic recombination found in T lymphocytes [90]. In addition to having a favorable epigenetic profile after reprogramming, PBMCs are less invasive to obtain than fibroblasts, and are exposed to fewer environmental mutagens. Also, PBMCs need less time in culture before reprogramming and generate colonies faster after reprogramming than fibroblasts [89].

### 1.4.2 Using iPSCs to study ALS

The reprogramming of fibroblasts from patients with fALS with a mutation in SOD1 into iPSC and subsequent motor neuron differentiation was first reported in 2008 [91]. Since then many types of fALS have been modeled using iPSCs from patient fibroblasts including TDP43 [92, 93], C9ORF72 [94, 95], and vamp-associated protein B/C (VAPB)[96]. Only one study to date has used iPSCs from sALS patients [97]. All of these studies describe the chemical characteristics of iPSC derived motor neurons, including immunostaining for the motor neuron transcription factors HB9 and Islet1, followed by expression of choline acetyltransferase (ChAT). Many also show functional characterization of ion channel and action potential formation by whole cell patch clamp.

There are data to suggest that these cells retain disease-causing mutations during reprogramming and display a phenotype similar to what is seen in patients.

Motor neurons differentiated from patient iPSCs with mutations in TDP43 conserved genetic mutations and increased vulnerability to cell stress [92, 93].

Recent findings suggest that iPSCs from fALS patients show some of the same characteristics of intrinsic hyperexcitability seen in the disease. ALS iPSC-derived motor neurons with mutations in three different genes displayed increased spontaneous firing when compared to healthy or isogenic controls [98]. Upon further investigation the authors found decreased magnitude of delayed-rectifier potassium currents but no change in sodium currents. Treatment with retigabine, an activator of delayed-rectifier potassium channels, decreased spontaneous firing and increased survival of ALS patient derived motor neurons [98].

Another study found that motor neurons derived from ALS patients with a hexanucleotide repeat in C9ORF72 are more susceptible to glutamate toxicity. This could be rescued by antisense oligonucleotides targeting C9ORF72 or by knockdown of an RNA binding protein, ADARB2. ADAR proteins mediate editing of the GluR2 AMPA receptor, making it calcium impermeable. Without this editing, as happens in sALS [99], AMPA receptors are calcium permeable and may contribute to excitotoxicity [95].

### 1.4.3 Mitochondrial regulation in hPSCs

Respiration analysis suggests that hPSCs produce the majority of ATP through anaerobic glycolysis compared to mitochondrial oxidative phosphorylation (OXPHOS) in somatic cells [100-103]. The details of this reversible switch remain unclear, and may vary between different cell lineages. Initial studies reported that hPSCs had few, underdeveloped mitochondria [104-106]. Recent studies have shown that while they rely on glycolysis for ATP production, hPSCs have active respiratory chain complexes

and respire at maximal capacity [100, 107]. Glycolysis is not as efficient at making energy but is faster and produces less ROS than OXPHOS. The switch to OXPHOS during differentiation would require increased mitochondrial respiratory capacity. There is evidence to suggest that this is achieved by an increase in mitochondrial mass, ATP and subsequent ROS production during spontaneous differentiation of hPSCs [108, 109]. This process is reversed during reprogramming of somatic cells into iPSCs.

Recent studies have started to shed light on the mechanisms underlying the switch from glycolysis to OXPHOS during cellular differentiation. One protein thought to be involved in this switch is uncoupling protein 2 (UCP2). UCP2 is a mitochondrial protein located in the inner membrane and is thought to uncouple the ETC from the production of ATP by allowing protons to leak through the membrane. The exact function of UCP2 remains unknown but recent findings implicate it in the metabolic change from glycolysis to OXPHOS during cellular differentiation by decreasing glucose utilization by mitochondria [110, 111]. UCP2 expression decreased during neuronal differentiation of mouse embryonic stem cells [112]. Hypoxia-inducible factor one alpha (HIF1α) is another protein that appears to be important for iPSC reprogramming. A recent study found increased HIF1α in undifferentiated cells and activation of HIF1α resulted in increased glycolysis and improved reprogramming [113].

### 1.4.4 Low oxygen conditions

Normal cell culture conditions grow cells in room air containing approximately 20% oxygen. This is much higher than what cells are exposed to in the developing or adult nervous system. Interstitial tissue oxygen levels in the mammalian brain range

from ~1-5% [114]. Low oxygen conditions (2-5%) have been shown to enhance proliferation, differentiation and survival of stem cells and neurons [115-118], including spinal motor neurons [117]. No ALS iPSC studies to date have used low oxygen conditions.

## 1.5 Aims of the study

The hypothesis to be tested in the current study states that differentiation of human pluripotent stem cells into electrically excitable motor neurons will result in increased mitochondrial biogenesis.

The specific aims are:

1. To generate motor neurons from hESC- and iPSC-derived human neural stem cells
2. To determine the effect of motor neuron differentiation on mitobiogenesis in human neural stem cells in 5% oxygen conditions
3. To examine the electrophysiological maturation of hPSC-derived motor neurons

# CHAPTER TWO

# GENERAL METHODS

## 2.1 Culture of hESC-derived hNSCs

GIBCO® Human Neural Stem Cells were purchased from Life Technologies (Grand Island, NY). These cells are derived from the NIH approved human embryonic stem cell line H9 (WA09) and retain a normal human female karyotype for multiple passages. They can be differentiated into neurons, oligodendrocytes, or astrocytes. To remain in an undifferentiated state cells were grown in KnockOut D-MEM/F-12 containing 2 mM GlutaMAX-I supplement, 20 ng/mL human recombinant basic fibroblast growth factor (bFGF) and epidermal growth factor (EGF) and 2% StemPro neural supplement up to passage 32. Medium was changed every 2-3 days and cells were maintained between 50 and 90% confluence. When cells were ~90% confluent they were dissociated using TrypLE™ and plated on culture vessels coated with CELLStart™. All cultures were grown at 37°C in 5% oxygen and 5% $CO_2$ conditions.

## 2.2 iPSC generation and neural induction

Peripheral blood was collected from one healthy male control patient, age 62, in accordance with a Virginia Commonwealth University IRB-approved protocol at the Parkinson's and Movements Disorder's Center. Integration-free iPSCs were generated from human peripheral blood mononuclear cells (PBMCs) using a previously described protocol[90], with modifications. Specifically, blood was collected in sodium citrate vacutainers and PBMCs were isolated using Ficoll-Paque Premium (GE Healthcare)

density gradient centrifugation within 4 hours of draw time. PBMCs were expanded by culturing for two weeks in PBMC medium that supports erythroblast expansion and eliminates lymphocytes. Lymphocytes were not used for reprogramming because of their high incidence of somatic rearrangements. The pEB-C5 and pEB-Tg plasmids were obtained from Addgene (Cambridge, MA) and grown in the VCU Macromolecular Core Lab. The pEB-C5 plasmid contains five reprogramming factors (OCT4, SOX2, KLF4, c-MYC, and Lin28) and the pEB-Tg plasmid contains the SV40 large T antigen that enhances reprogramming efficiency. $3x10^6$ PBMC were electroporated with the plasmids using an Amaxa Nucleofector 4D (Lonza, Allendale, NJ). This technique uses electrical pulses to permeabilize the cell membrane in order to allow the plasmid access to the cytosol. Immediately following electroporation an equal volume of 37 °C RPMI medium was added to the cuvette and the cells allowed to recover for 10 min at 37 °C before returning to culture in PBMC medium. Transfected cells were co-cultured on mouse embryonic fibroblasts beginning at day 2 and the schedule of medium changes outlined in the protocol were followed. On day 14 maintenance medium was changed to mTeSr (Stem Cell Technologies, Vancouver, BC) and colonies with PSC morphology were picked to wells of a 96 well plate beginning at about day 21. Viable colonies were expanded in mTeSR medium on Geltrex (Life Technologies, Grand Island, NY) coated plates at 37° C in a humidified CO2 incubator with the oxygen level held at 5%. Growth medium supplemented with 10 uM ROCK inhibitor Y27632 (R&D Systems, Minneapolis, MN) was used for the first 24 hours after colonies were split.

Neuralization of iPSCs was accomplished using PSC Neural Induction Medium (Life Technologies) according to protocol [119] with modifications. This protocol allowed

for a faster, less labor-intensive, and consistent neural induction protocol. Briefly, iPSC colonies were maintained in PSC Neural Induction Medium beginning at day 1 after splitting. On day 5 colonies with good morphology were picked to fresh Geltrex coated dishes and induction continued for another 5 days. On day 10 colonies were detached using Accutase (Life Technologies), passed through a 100 um strainer, centrifuged at 300 x g for 4 min. and plated in neural expansion medium on Geltrex coated dishes. Cultures were maintained at 37° C in a humidified CO2 incubator with the oxygen level held at 5%. Growth medium supplemented with 10 uM ROCK inhibitor Y27632 (R&D Systems, Minneapolis, MN) was used for the first 24 hours after the neural stem cells were split through passage 4.

2.3 Differentiation of hNSCs into motor neurons

For differentiation of hESC-derived hNSCs into motor neurons media was changed to neurobasal medium containing 2% B-27 serum-free supplement and 2 mM GlutaMAX-I supplement plus 0.1 μM retinoic acid (RA) for 7 days followed by 7-21 days of 0.1 μM RA plus 0.5 μM purmorphamine (PM) [117, 120-126]. Media was changed every 2-3 days and cultures received half media changes except on days 0 and 7, when cultures received full media changes. RA and PM concentrations and timing were chosen based on previous studies [120, 127].

After neural induction, iPSCs were differentiated as described previously, with some modifications [128]. Briefly, adherent cells were grown in neural induction media containing DMEM/F12 with 0.2 μM LDN-193189 (LDN; Stemgent), 10 μM SB431542 (SB; Stemgent), 10 ng/ml BDNF (R&D systems), 0.4 ug/ml L-ascorbic acid (Sigma), 2

mM GlutaMAX-I supplement, 1% N-2 supplement, and 1% nonessential amino acids (NEAA). Two days later 1 μM RA was added. On day four LDN/SB was stopped and 1 μM smoothened agonist (SAG; Calbiochem or Santa Cruz) and 0.5 μM PM were added. On day 14 cells were switched to neurobasal media containing 2 mM GlutaMAX-I, 2% B-27, 1% NEAA, 0.4 ug/ml AA, 10 ng/ml GDNF (R&D), 10 ng/ml CNTF (R&D). Media was replaced every 2-3 days. Unless otherwise specified, all cell culture materials were purchased from Life Technologies. All cultures were grown at 37°C in 5% oxygen and 5% $CO_2$ conditions.

2.4 Nucleic acid isolation and cDNA synthesis

For qPCR analysis of hESC-derived cells DNA and RNA were extracted at seven-day time points through day 28 using the AllPrep DNA/RNA Mini Kit (Qiagen) according to manufacturer instructions. In order to achieve increased yield and quality, for iPSC-derived cells RNA was extracted at D0 and D21 with the RNeasy or RNeasy Plus Micro Kit (Qiagen) and DNA was extracted with the DNeasy Blood and Tissue Kit (Qiagen) according to manufacturer instructions. Quantification of isolated DNA and RNA was performed using a Nanodrop 2000c spectrophotometer (Thermo Scientific). RNA was reverse transcribed into cDNA using the iScript or iScript Advanced cDNA synthesis kit (BioRad) which uses both random hexamer and oligo dT primers, following the manufacturer's protocol.

2.5 Quantitative PCR

For qPCR, 25-50 ng cDNA or 0.1 ng of DNA per well was loaded into a 96-well plate and analyzed with the CFX-96 Real-Time PCR Detection System (BioRad) using relative quantitation methods. All samples were analyzed in triplicate. Neuronal markers (NEFL, MAP2, and TUBB3), TFMB2, and mtDNA-encoded genes (12s rRNA, ND2, CO3, ND4) were measured using a multiplex qPCR assay. Endogenous reference genes (TOPO1, 14-3-3-Z, GAPDH, B2M, CYC1, AND UBC), pluripotency genes (KLF4, CMYC, LIN28, OCT4, SOX2) mitochondrial biogenesis genes (PGC-1α, POLG, POLRMT, TFAM, ERRα, NRF1, NRF2), glial markers (GL1-1 and GFAP), NSE was measured individually using EvaGreen PCR. Primers for PGC-1α were specifically designed in a region to detect all major isoforms. Primer sequences can be found in **Figure 3**. Reagents included SsoFast EvaGreen® Supermix (BioRad) and primers designed with Beacon Designer software (Premier Biosoft international, Palo Alto, CA) and supplied by Eurofins MW Operon (Huntsville, AL). PCR conditions were 30 seconds at 95 °C, followed by 40-45 cycles of 10 seconds at 95 °C and then 15 seconds at $T_m$ (primers) -5 °C. Melt curve analysis was used to verify primer specificity, and efficiency was determined using standard curve analysis of commercially available human fetal brain total RNA (Clontech, Mountain View, CA).

All gene expression analysis were conducted using the qbasePLUS® relative quantitation method (Biogazelle qbasePLUS®, http://www.biogazelle.com), which is a modification of the ΔΔCq method that allows normalization with multiple reference genes. Data was normalized to the geometric mean of two reference genes determined

to have the greatest stability using the software qbasePLUS-GeNorm (BioGazelle; 14.3.3.Z and CYC1 for cDNA and CYC1 and GAPDH for gDNA for both cell types).

| MtDNA encoded genes | | |
|---|---|---|
| ND2 | PROBE | [6-FAM]CACGCAAGCAACCGCATCCATAAT[BHQ1a-Q] |
| ND2 | SP | AAGCTGCCATCAAGTATTTCC |
| ND2 | ASP | GTAGTATTGGTTATGGTTCATTGTC |
| | | |
| COX3 | PROBE | [5TET]CGAAGCCGCCGCCTGATACTG[BHQ1a-Q] |
| COX3 | SP | TTTCACTTTACATCCAAACATCAC |
| COX3 | ASP | CAATAGATGGAGACATACAGAAATAG |
| | | |
| ND4 | PROBE | [AminoC6+TxRed]AGCCAGAACGCCTGAACGCAG[BHQ2a-Q] |
| ND4 | SP | TGGCTATCATCACCCGATG |
| ND4 | ASP | GGTGTTGTGAGTGTAAATTAGTC |
| | | |
| 12SrRNA | PROBE | [Cy5]CGCCAGAACACTACGAGCCACAG[BHQ3a-Q] |
| 12SrRNA | SP | CCTCAACAGTTAAATCAACAAAAC |
| 12SrRNA | ASP | CTGAGCAAGAGGTGGTGAC |

| Mitobiogenesis genes | | |
|---|---|---|
| POLg | SP | TGGTCAAACCCATTTCACTG |
| | ASP | AGAACACCTGGCTTTGGG |
| | | |
| ERRa | SP | CTTCGCTCCTCCTCTCATC |
| | ASP | CTGGAGTCTGCTTGGAGTTAT |
| | | |
| NRF1 | SP | TTTGTATGCCTTTGAAGAT |
| | ASP | AACCTGGATAAGTGAGAC |
| | | |
| NRF2 | SP | GTTACAACTAGATGAAGAGACA |
| | ASP | ATCCACTGGTTTCTGACT |
| | | |
| TFAM | SP | AATCTGTCTGACTCTGAA |
| | ASP | CACATCTCAATCTTCTACTT |
| | | |
| TFMB2 | SP | GTATCTTATTCAAATGATTCCTC |
| | ASP | TAAGTGGTCTATTACAGTGG |
| | Probe | [5TET]ACCAAGA...AACT[BHQ1a-Q] |
| | | |

| | | |
|---|---|---|
| PGC1a | SP | GATGTGAACGACTTGGAT |
| | ASP | TTGAAGGCTCATTGTTGTA |
| | | |
| POLRMT | SP | AAGATACTGGAGAAGGATAAGC |
| | ASP | GCTCTGGAATGGCATCTG |
| | | |
| Isl1 | SP | GTTGGAGAAAGTGGGAAAT |
| | ASP | CTACCATATCACCTTGTCATT |
| | | |
| VACht | SP | ACTCCTCAACCTTGACTTC |
| | ASP | CCATTGGACAAGAGAGAAAG |
| | | |
| HB9 | SP | GTGAGAAGAACCGACCCACC |
| | ASP | CTCCAGAGGCGGTTTCAAGT |

| **Reference genes** | | |
|---|---|---|
| TOPO1 | SP | TGAGCCAGATAACAAGAA |
| | ASP | TTGATGCCTTCAGGATAG |
| | | |
| 14-3-3-Z | SP | GTAGACCATTTGTCATCCAT |
| | ASP | AGAAGTAACATAAACCTGTCATA |
| | | |
| CYC1 | SP | ACTGCGGGAAGGTCTCTA |
| | ASP | TGCCATCGTCAAACTCTAAG |
| | | |
| B2M | SP | TATCCAACATCAACATCT |
| | ASP | TTCCAATAATCCTGTCAA |
| | | |
| UBC | SP | ATTTTAGGACGGGACTTG |
| | ASP | CGAGAAGGGACTACTTTT |
| | | |
| GAPDH | SP | GTCGGAGTCAACGGATTT |
| | ASP | CAACAATATCCACTTTACCAGAG |

| **Pluripotency genes** | | |
|---|---|---|
| KLF4 | SP | CCTTGCTGATTGTCTATT |
| | ASP | AAGTCAACGAAGAGAAGA |
| | | |
| CMYC | SP | CGCATCCACGAAACTTTG |
| | ASP | CTTGCTCGGGTGTTGTAA |
| | | |
| LIN28 | SP | CCAGAGTGAAATGATTAAGTA |
| | ASP | GAGGATACAAGATGTGAAAA |
| | | |

| | | |
|---|---|---|
| OCT4 | SP | AGGAAGCTGACAACAATG |
| | ASP | TGGTTCGCTTTCTCTTTC |
| | | |
| SOX2 | SP | ATGGTTGTCTATTAACTTGT |
| | ASP | TCTCTCCTCTTCTTTCTC |

| **Neuronal genes** | | |
|---|---|---|
| NEFL | SP | CTCCCGAAATCAGGTCAA |
| | PROBE | [5-FAM]CCATCACCAACCAACCAACCAG[BHQ1a-Q] |
| | ASP | GAGGAAATTCATAGCACAACA |
| | | |
| MAP2 | SP | CAGGAGACAGAGATGAGAA |
| | PROBE | [5TET]ACAGTTCTATCTCTTCTTCAG[BHQ1a-Q] |
| | ASP | GGAGTGATGGCAGTAGAC |
| | | |
| TUBB3 | SP | CATCCAGGAGCTGTTCAA |
| | PROBE | [AminoC6+TxRed]CGCATCTCCGAGCAGTTCAC[BHQ2a-Q] |
| | ASP | GTCGTTCATGTTGCTCTC |
| | | |
| NSE | SP | TGAGGGATGGAGACAAAC |
| | ASP | GAGACCTGAGCTGATGAG |

| **Glial genes** | | |
|---|---|---|
| GFAP | SP | CCGTCTGGATCTGGAGAG |
| | ASP | TCCTCCTCGTGGATCTTC |
| | | |
| GLT-1 | SP | GACAGTCATCTTGGCTCAG |
| | ASP | GAGCAGCAGATTCTTCCC |

**Figure 3. Primer sets used in the present study** including sense (SP) and antisense primers (ASP). For multiplex assays, probe sequences are given.

## 2.6 mtDNA copy number

MtDNA copy number was determined using a four-color multiplex qPCR assay targeting human mtDNA-encoded genes around the mitochondrial genome (12s rRNA, ND2, CO3, ND4). Absolute quantification of DNA samples was based on human mtDNA copy number standards run on the same plate. The mtDNA standards were prepared as described previously [129]. Briefly, human genomic DNA was purchased from Roche and treated with limiting amounts of Plasmid-Safe ATP-dependent DNase (Epicentre Biotechnologies, Madison, WI) according to manufacturer recommendations. This procedure selectively digests all forms of DNA but does not affect closed circular or nicked circular double-stranded DNA, leaving only circular mtDNA. MtDNA was further purified according to protocols for the UltraClean GelSpin DNA purification kit (MO BIO Laboratories, Calsbard, CA) and quantified with a DNA Quant-iT assay kit (Invitrogen, Calsbard, CA) and the linear band was visualized on a 0.8% agarose gel.

## 2.7 Confocal microscopy and immunofluorescence

For immunocytochemistry analysis cells were seeded in 35 mm glass bottom confocal dishes. On D21 cells were fixed in 4% paraformaldehyde and 4% sucrose in PBS at room temperature for 15 minutes. Cells were incubated for 60 minutes in blocking buffer (5% goat serum, 1% BSA, 0.1% Triton-X in PBS). Cells were incubated overnight at 4°C with primary antibody (1:100) diluted in 5% goat serum. Primary antibodies included rabbit anti-ChAT (Millipore), mouse anti-nestin (abcam), mouse anti-TOMM20 (abcam), mouse anti-Isl1/2 and HB9 (MNR2; DHSB), and rabbit anti-MAP2 (Millipore). Alexa Fluor conjugated secondary antibodies (1:400, Life Technologies)

were added for 60 minutes at room temperature. After washes, VECTASHIELD mounting media with DAPI was added for visualization of nuclei. Images were obtained with an Olympus FV1000 confocal microscope. For TOM20 and percent positive quantitation, ten representative fields were taken and analyzed using MetaMorph image analysis software (Molecular Devices). For TOMO20 staining pixel values were normalized to number of cells in each image, identified by DAPI nuclear staining.

2.8 Western blot analysis

Cell homogenates were prepared by dissociating cells with TrypLE™ and washing three times with PBS. After the last wash samples were resuspended in RIPA buffer (50 mM Tris-HCl, 1% NP-40, 0.25% Na deoxycholate, 150 mM NaCl, 1 mM EGTA, 1 mM Na orthovanadate, 1 mM Na fluoride, pH 7.4) with 10 ul/ml Protease Inhibitor Cocktail Set I (Calbiochem) and 10 ul/ml of 100 mM PMSF (Sigma), followed by water bath sonication for 2 minutes. Samples were incubated on ice for 30 minutes and vortexed every 5 minutes prior to centrifugation at 15,000 x g for 10 minutes at 4°C to remove cellular debris. The supernatant was transferred to a new microcentrifuge tube and stored at -20°C for later analysis.

Equal concentration (20-25 ug) of total cell protein from each sample was separated on a 4-12% Bis-Tris Criterion precast gel at 200 V for 1 hour using sodium dodecyl sulfate-polyacrylamide gel electrophoresis (SDS-PAGE). The proteins were transferred to nitrocellulose membranes using the iBlot transfer system (Invitrogen). After blocking the membrane for 1 hour with Odyssey® blocking buffer (LI-COR Biosciences) the membrane was probed primary antibody overnight at 4°C. Primary

antibodies were diluted in blocking buffer with 0.1% Tween 20 and included the MitoProfile® Total OXPHOS Human WB Antibody Cocktail (1:200, ab110411, Abcam), mouse anti-VDAC1 (1:1000, Abcam), and rabbit anti-beta actin (β-actin; 1:500, Abcam). The membrane was probed with 800CW goat anti-mouse or 680 goat anti-rabbit secondary antibodies (1:15000, LI-COR) at RT for 1 hour and band intensity was quantified using the Odyssey infrared imaging system (LI-COR, Lincoln, NE).

### 2.9 XF24 extracellular flux analyzer

Cell metabolic rates were measured using an XF24 Extracellular Flux Analyzer (Seahorse Bioscience) in unbuffered DMEM, pH 7.4 as described previously by our group [130]. Briefly, on day 16 cells were seeded onto an XF24 Cell Culture Microplate (Seahorse Bioscience) at 60,000 cells/well with 10 μM Y-27632 dihydrochloride, a selective inhibitor of Rho-associated protein kinase (ROCK; Tocris) and incubated at 37°C in 5% oxygen. After 3 days hNSCs were seeded onto the same XF24 Cell Culture Microplate at 40,000 cells/well with 10 μM ROCK inhibitor and incubated at 37°C 5% oxygen for 24 hours. iPSC-derived cells (D0 and D21) were plated at 60,000 cells/well the day before recording. Each cell type was tested at three to four concentrations to determine the most reliable plating density. Inhibitors included oligomycin (1 μM) and FCCP (0.5-1 μM). OCR and ECAR were normalized to protein concentration (Micro BCA Kit, Pierce) for all experiments to account for differences in cell size.

## 2.10 Lentiviral generation and infection

For generation of the HB9::GFP lentivirus services and products generated by the VCU Massey Cancer Center Biological Macromolecule Shared Resource, supported, in part, with funding from NIH-NCI Cancer Center Support Grant P30 CA016059 were used. Addgene plasmid 37080 [124] was cotransfected with packaging and envelope plasmids cCMVR8.74 and MD2G. Transfection and viral concentration were performed using standard published protocols. Virus titer was 5 x 10^7 TU/mL in PBS. Cells were infected at a multiplicity of infection (MOI) of 3-5 with 8 ug/ml protamine sulfate 5 days before recording.

## 2.11 Electrophysiology

For whole-cell patch-clamp experiments cells were differentiated for 28 days. Two days before recording cells were moved to 12 mm diameter circular glass coverslips (neuvitro). On the day of recording coverslips were placed in a recording chamber on the stage of an inverted microscope (Olympus). An Axopatch 200B amplifier (Molecular Devices) and pClamp 10 software (Axon Instruments) were used to record whole-cell currents. Patch pipettes were pulled from thick-walled borosilicate glass capillaries to resistances of 2-4 mΩ and filled with internal solution containing 120 mM KCl, 2 mM $MgCl_2$, 1 mM $CaCl_2$, 10 mM EGTA, 10 mM HEPES, 2 mM $Na_2ATP$ (pH 7.2). Extracellular solution consisted of 135 mM NaCl, 5 mM KCl, 2 mM $MgCl_2$, 1 mM $CaCl_2$, 10 mM HEPES, and 10 mM glucose (pH 7.4). Action potential threshold was determined as the voltage at which the d(V)/d(T) function deviated from zero. Action

potential height was determined by measuring the threshold to the peak of the action potential.

## 2.12 Statistical analysis

All results are expressed as the mean ± standard error of the mean (SEM). The number of experiments performed is denoted by n. Outliers were excluded at the $p<0.05$ level by Grubbs' test. Statistics were calculated using one-way ANOVA or unpaired t-test in Prism software (GraphPad, Prism). P-values $<0.05$ were considered statistically significant.

# CHAPTER THREE

## Generation of motor neurons from embryonic and iPSC-derived human neural stem cells

### 3.1 Rationale and Hypothesis

The present study tested the ability of factors crucial for the patterning of motor neurons in the developing spinal cord to differentiate human neural stem cells (hNSCs) into motor neurons in culture. This will allow for the study of a cell type currently only accessible in post mortem tissue or in animal models. Additionally, reprogramming cells from patients may prove beneficial in the modeling of complex diseases with no single genetic cause, including ALS. Since iPSCs have the same genetic profile as living patients they may replicate disease pathology. There is evidence that disease processes begin decades before symptom onset, so these 'young' cells may give us insights into disease mechanisms.

Previous studies have differentiated hESCs and iPSCs derived from fibroblasts into motor neurons [91-97, 128, 131-134]. As summarized in **Figure 4**, this study uses human embryonic stem cells (hESCs) and induced pluripotent stem cells (iPSCs) from healthy individuals and lays the groundwork for replicating these studies using patient cells. Peripheral blood mononuclear cells (PBMCs) were used for reprogramming instead of fibroblasts (**Figure 4**). iPSCs derived from PBMCs display an epigenetic profile closer to hESCs than iPSCs derived from fibroblasts [89] and PBMCs are exposed to fewer environmental mutagens. Previous studies have shown that PBMCs can be reprogrammed into iPSCs but it remains to be shown if they can differentiate into motor neurons.

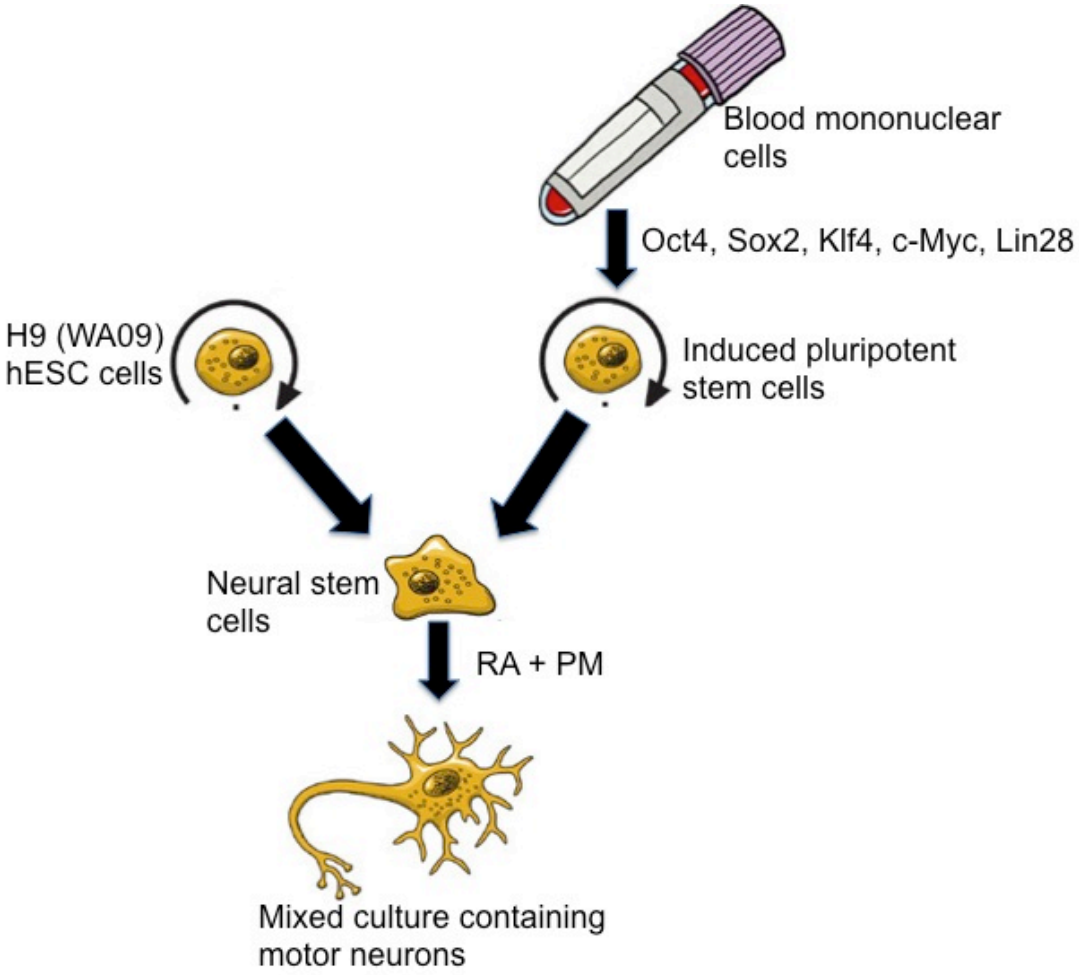


**Figure 4. Schematic of motor neuron differentiation.** Neural stem cells from hESC and iPSC-derived cells will be differentiated into motor neurons

## 3.2 Statement of contributions

This chapter contains data collected by three individuals. Amy Ladd generated that data represented in Figure 5 showing mtDNA encoded gene expression in ALS and control PBMCs. This figure was reproduced from a recent publication from our lab [26]. For iPSC generation Amy Ladd and I isolated PBMCs from peripheral blood and Paula Keeney performed all of the cell culture work to generate the iPSC cell line (Figure 6 and 7B). I performed all cell culture and experiments with the H9 hESC-derived cell line and the iPSC cell line after neural induction (Figures 7A, 9, and 10)

## 3.3 Results

### 3.3.1 Generation of iPSCs from PBMCs.

Peripheral blood samples from nine sporadic ALS (sALS) patients and 11 controls were collected according to an IRB approved protocol. If possible, spouses were used as controls. This allowed for a convenient, relatively age-matched, gender balanced control group. Additionally, these individuals likely lived together and would therefore be exposed to a similar environment. Although ALS iPSCs are not used in this study, isolated PBMCs are frozen for future reprogramming use from all patients.

Following isolation, PBMCs were cultured for two weeks in conditions favoring erythroblast expansion and eliminating lymphocytes. This is an important step, as lymphocytes (70-90% of PBMCs) commonly rearrange their DNA and thus stem cell lines derived from them may have an increased rate of forming lymphomas [135]. Additionally, this culture protocol enriches for CD34+ hematopoietic stem cells without the need for cell sorting. Interestingly, PBMCs from ALS patients have decreased

mitochondrial DNA encoded gene expression compared to controls [26]. This mirrors what is seen in post mortem spinal cord from sALS patients[26] and may suggest a systemic bioenergetic impairment in these individuals. These findings, along with decreased growth rates and survival of the sALS iPSC cell lines support the hypothesis that ALS cells may be more sensitive to stress, as seen in familial ALS (fALS) derived cells [93].

As described in **Figure 4**, after expansion, PBMCs were reprogrammed into iPSCs by electroporation of five reprogramming factors, Oct4, Sox2, Klf4, c-Myc, and Lin28 as well as a plasmid containing the SV40 large T antigen. As shown in **Figure 5A**, two weeks after reprogramming live cells express TRA-1-60, a human stem cell antigen and early marker of pluripotency. As iSPC colonies formed, starting at day 21, they were identified and expanded. To confirm pluripotency of the iPSC cell line, three colonies were chosen for qPCR analysis. **Figure 5B** shows increased expression of genes encoded by the reprogramming plasmid including Oct4, Sox2, and Lin28 in iPSC colonies compared to PBMCs (**Figure 5B**; *$p<0.05$, **$p<0.01$).

After 10 days in neural induction media, NSC colonies were picked and expanded. qPCR revealed decreased expression of the plasmid encoded genes Oct4, Sox2, and Lin28 in NSCs (**Figure 5B**; *$p<0.05$, **$p<0.01$). This suggests that the plasmid is no longer being expressed.

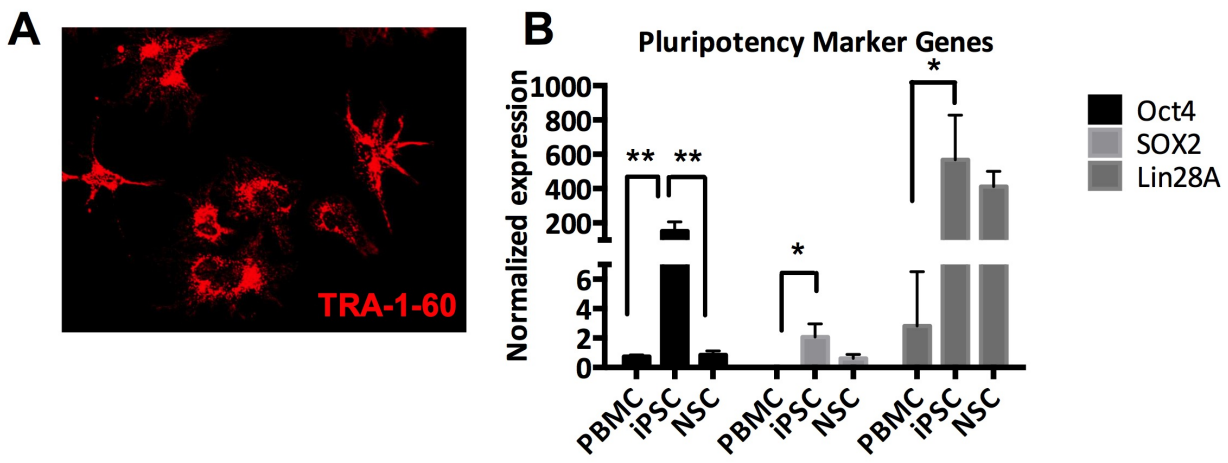


**Figure 5. Generation of iPSCs from blood** A) Expression of TRA-1-60, an early marker of pluripotency, after reprogramming B) Expression of genes encoded by the reprogramming plasmid in peripheral blood mononuclear cells (PBMCs), induced pluripotent stem cells (iPSCs), and neural stem cells (NSCs) (*p<0.05, **p<0.01). SOX2 expression was undetectable in PBMCs

### 3.3.2 Neural induction of iPSCs

In order to confirm successful neural induction of iPSCs, cells were stained with the human neural stem cell (hNSC) marker, nestin. Nestin is an intermediate filament protein expressed in neuroepithelial precursors that become neurons and glia [136]. A representative confocal image is shown in **Figure 6A**. 67% of cells stained positive for nestin. To test if iPSC-derived hNSCs display an early commitment to a particular lineage, expression of a panel of neuronal and glial genes were assessed by qPCR. Neuronal markers neural filament light chain (NEFL), microtubule-associated protein 2 (MAP2), and beta III tubulin (TUBB3) increased expression during neural induction (**Figure 6B**; *$p<0.05$).

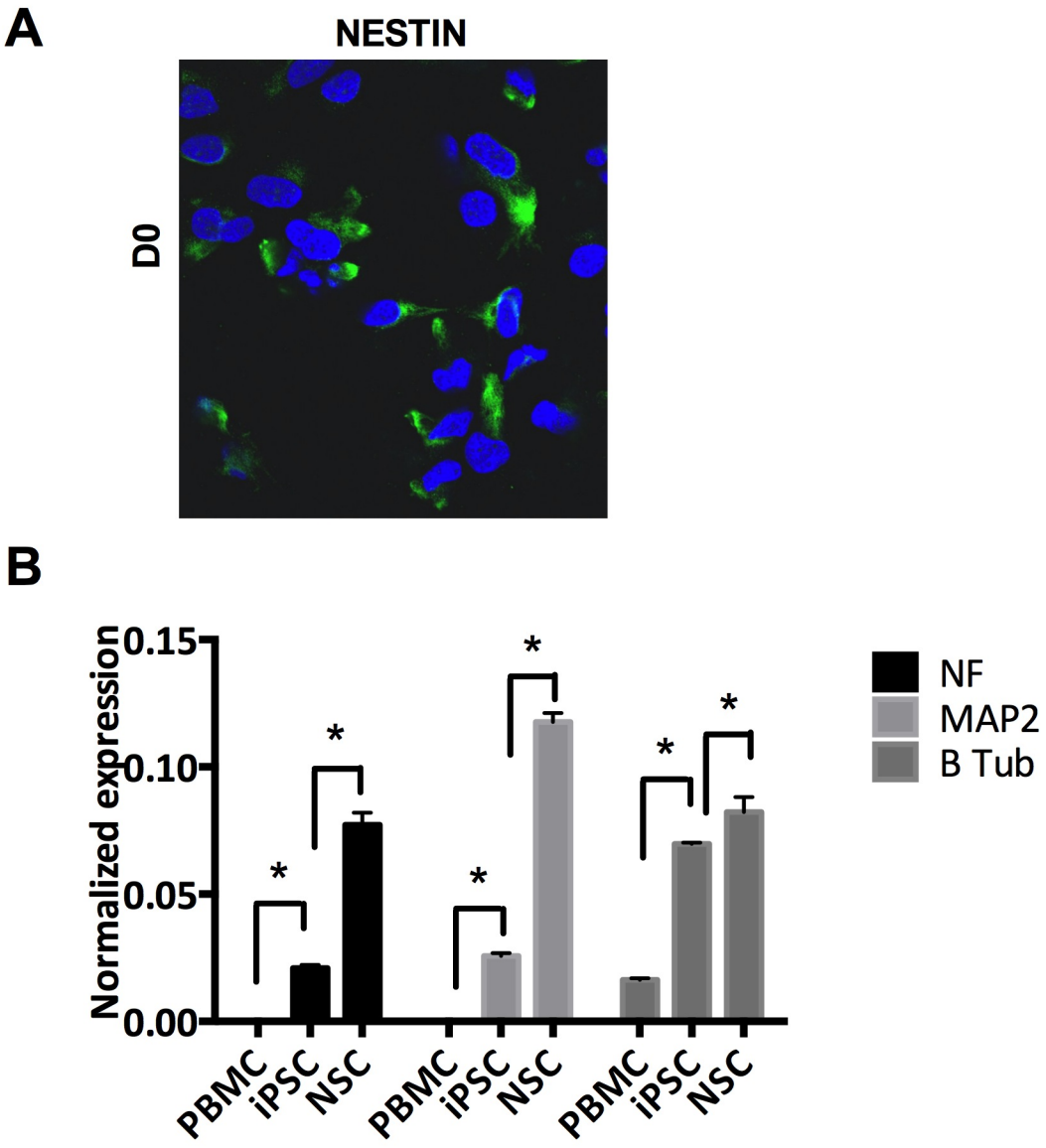


**Figure 6. Neural induction of iPSCs.** A) A representative confocal image showing expression the neural stem cell marker nestin (green) and DAPI nuclear staining (blue) after neural induction B) qPCR analysis of neuronal markers in iPSCs and after neural induction (*p<0.05)

### 3.3.3 Spontaneous differentiation of NSCs into neurons, astrocytes and oligodendrocytes

While the iPSC cell line was being established, experiments were performed using commercially available hNSCs. The hNSC line used is derived from NIH approved H9 (WA09) hESC cells. These cells have a normal human female karyotype and can remain in an undifferentiated state in the presence of growth factors or can differentiate into neurons, astrocytes or oligodendrocytes. Starting from hNSCs instead of hESCs allowed for an accelerated differentiation protocol since neural induction had already been completed. In addition, these cells are easier to culture since they are adherent, compared to hESC and iPSCs, which are often cultured and differentiated as floating embroyid bodies. Over 90% of these cells stained positive for the neural stem cell marker nestin on day 0 (D0; **Figure 7**). Many D0 cells also stained positive for the neuronal marker MAP2 but did not stain positive for the glial markers GalC or GFAP (**Figure 7**).

In order to test the differentiation capacity of hNSCs, growth factors bFGF and EGF were withdrawn from cell culture media for 14 days. This resulted in loss of nestin staining and spontaneous differentiation of cells into neurons (MAP2+), oligodendrocytes (galactocerebroside, GalC+), and astrocytes (GFAP+; **Figure 7**).

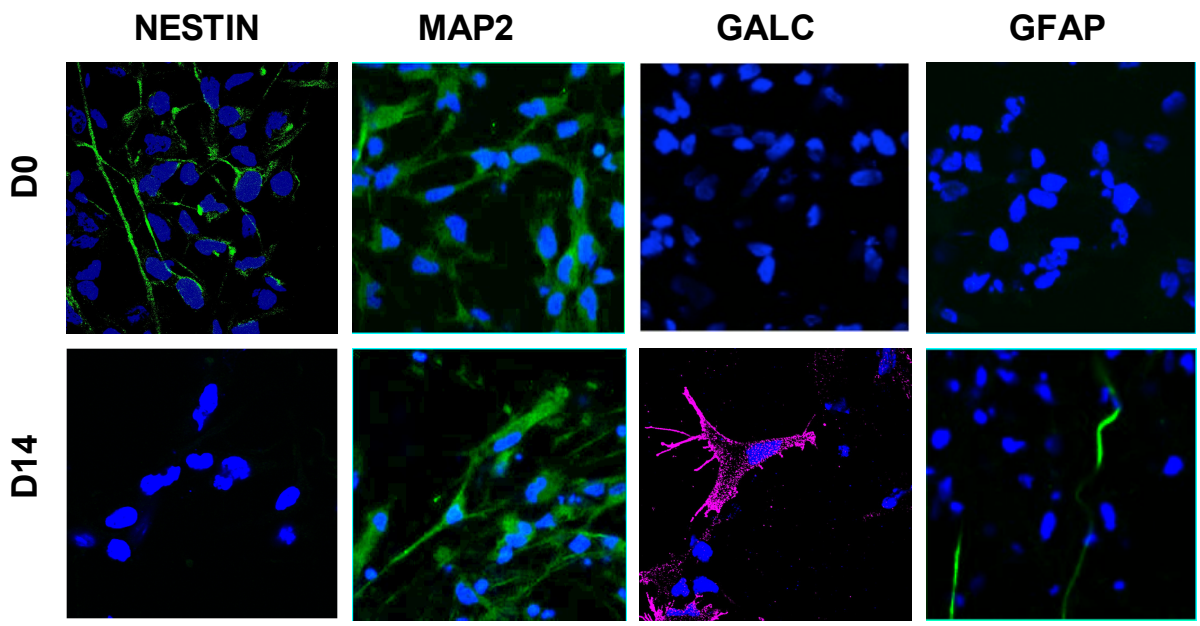


**Figure 7. Neuronal and glial markers after spontaneous differentiation.** Expression of the neural stem cell marker nestin, the neuronal marker MAP2, and the glial markers GALC and GFAP at day 0 (D0) and day 14 (D14) after spontaneous differentiation in hESC-derived cells

### 3.3.4 Motor neuron differentiation of hESC-derived cells

To test the ability of commercially available hNSCs to differentiate into specialized cell types we induced motor neuron differentiation with retinoic acid (RA) and purmorphamine (PM), a sonic hedgehog (SHH) agonist. SHH has been shown to regulate ventralization of neural tissues [35]. As shown in **Figure 8A**, qPCR analysis revealed that after 21 days of differentiation (D21) cells significantly increased expression of post mitotic motor neuron genes ISL1 and HB9 (t-test D0 vs D21, *p<0.05, **p<0.01). Phase contrast images on D21 revealed morphological changes including an extensive network of processes (**Figure 8B**). On D21 46% of cells stained positive for both MAP2 and HB9 and 51% stained positive for MAP2 and ISL1/2 (**Figure 8C**). GFAP staining was not observed in these cultures. Collectively, these findings suggest that cells acquire a motor neuron molecular phenotype by D21. Analysis comparing different passage numbers revealed that higher passage numbers resulted in more variable gene expression data, therefore all data were generated from cells with passage numbers less than 33.

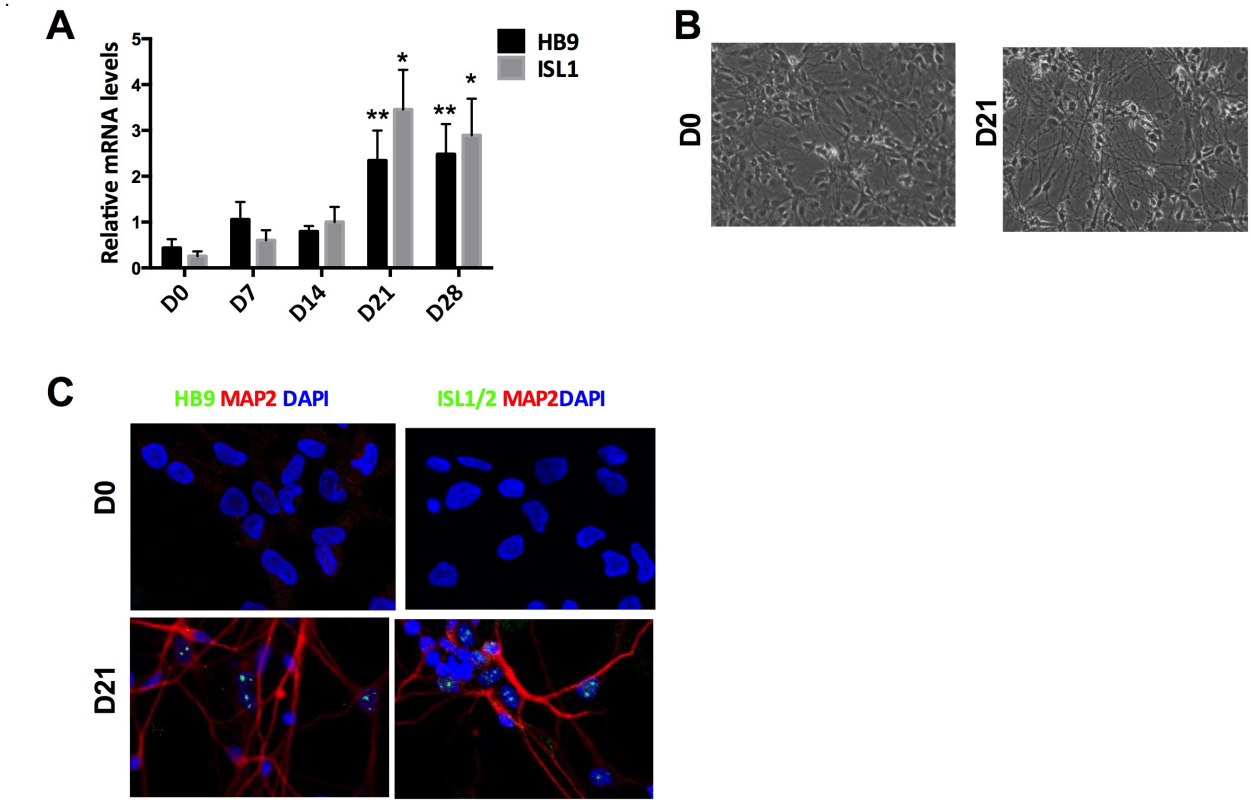


**Figure 8. Motor neuron differentiation of hESC-derived hNSCs.** A) qPCR expression of spinal motor neuron markers HB9 and ISL1 on day 0-28 (D0-D28) of motor neuron differentiation (*p<0.05, **p<0.01) B) Representative phase contrast images of D0 and D21 cells C) Immunostaining of MAP2 (red), HB9 or ISL1 (green), and DAPI (blue) on D0 and D21

3.3.5 Differentiation of motor neurons from iPSC-derived cells

For motor neuron differentiation of iPSC-derived cells the protocol was modified based on a recent publication [128]. The differentiation schematic is shown in **Figure 9A**. RA and PM concentrations remained the same, but small molecules SB435142 (SB) and LDN193189 (LDN) were used to induce neuralization by inhibition of SMAD signaling. Smoothened agonist (SAG) was added in addition to PM to further increase sonic hedgehog signaling. For increased neurotrophic support, GDNF and CNTF were added after day 14. Preliminary data revealed wide variations in gene expression in cells of different passage number; therefore all cells were cultured for a minimum amount of time, 4-6 days after thawing, before motor neuron differentiation was started. **Figure 9B** shows representative phase contrast images of D0 and D21 cells and is very similar to what was seen in hESC-derived cells. Expression of motor neuron markers HB9 and ISL1 were undetectable in D0 cells by qPCR and increased significantly on D21 (**Figure 9C;** $^{**}p<0.01$, $^{***}p<0.001$). The expression of vesicular acetylcholine transporter (VACHT) was also significantly increased on D21 compared to D0, suggesting that these cells are cholinergic neurons (**Figure 9C**). To further confirm motor neuron identity, cells were stained with HB9, ISL1/2, and MAP2. **Figure 9D** shows staining for these markers on D21 but not on D0.

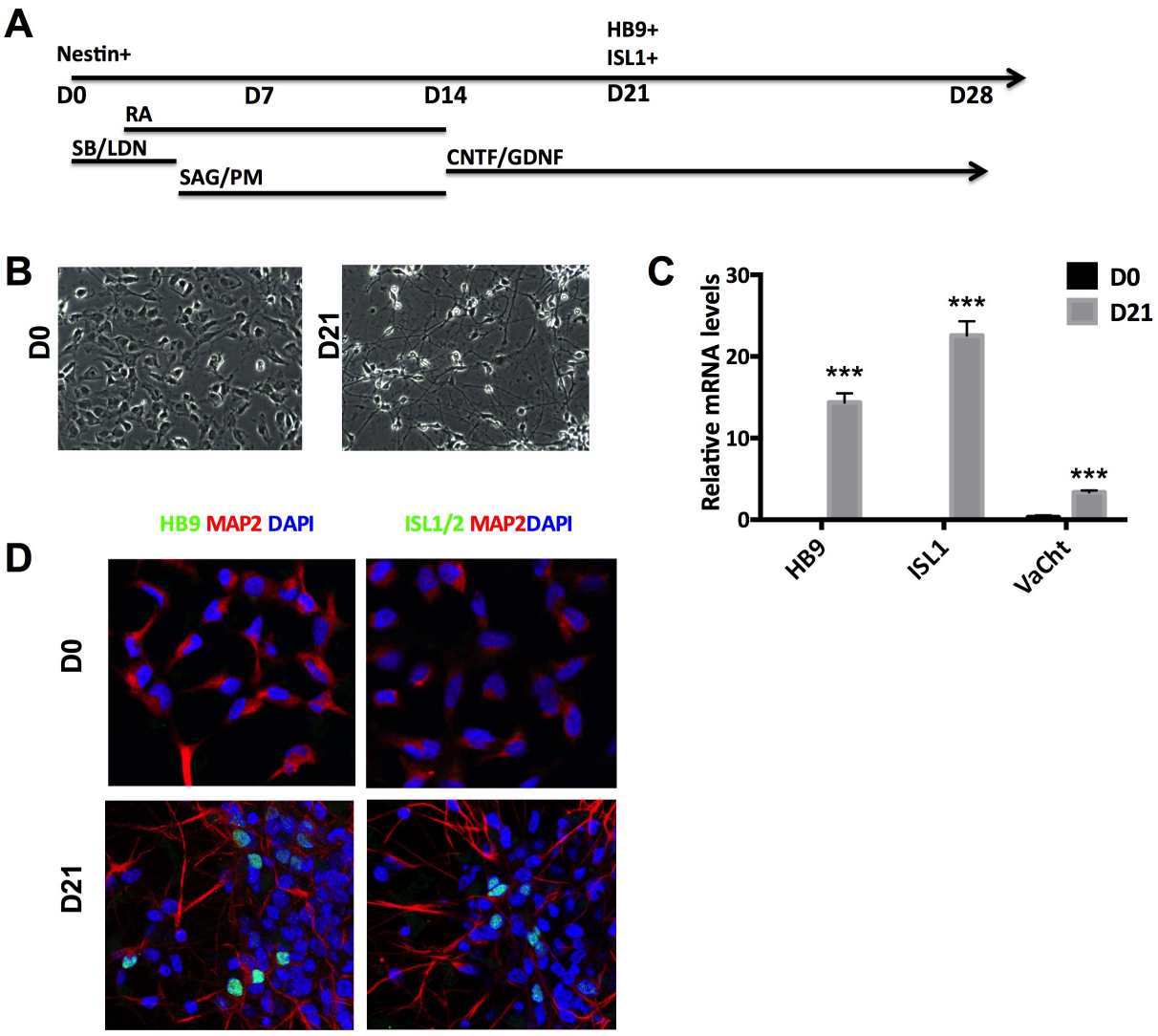


**Figure 9. Motor neuron differentiation of iPSC-derived hNSCs.** A) Schematic of the motor neuron differentiation protocol showing timing of neuralization with SB and LDN, caudalization with RA, induction of sonic hedgehog signaling with SAG and PM, as well as neurotrophic support from day 14 on with CNTF and GDNF B) Representative phase contrast images of D0 and D21 cells C) Expression of motor neuron genes HB9, ISL1, and VACHT (**p<0.01, ***p<0.001) D) Immunostaining of MAP2 (red), HB9 or ISL1 (green), and DAPI (blue) on D0 and D21

## 3.4 Summary

In summary, these studies demonstrate the ability to generate iPSC cell lines from PBMCs without viral expression or DNA integration of plasmid. The finding of decreased mtDNA encoded gene expression in sALS PBMCs suggests that these cells may replicate disease pathology since this mirrors what is seen in post mortem spinal cord from sALS patients. Secondly, commercially available hNSCs were differentiated into multiple neuronal cell types, including motor neurons. This accelerated protocol, without the need for suspension culture, may prove to be advantageous in labs without access to or experience with culturing stem cells. Finally, iPSCs were successfully induced to become motor neurons, based on multiple gene and protein markers. These cells may be used to understand human motor neuron physiology. Collectively, these studies set the stage for the study of human motor neurons and reprogramming and differentiation of ALS patient cells in the future.

# CHAPTER FOUR

## Mitochondrial biogenesis increases as cells differentiate from neural stem cells into motor neurons

### 4.1 Rationale and Hypothesis

Previous studies have demonstrated that both hESCs and iPSCs produce ATP mainly through glycolysis and that during differentiation there is a switch to energy production by oxidative phosphorylation (OXPHOS). The mechanism underlying this switch remains unknown, but an increase in mitochondrial mass, mtDNA copy number and ATP production has been seen during spontaneous differentiation of hESCs into all three germ layers [108, 109]. Based on these findings, this series of experiments hypothesized that mitochondrial biogenesis would increase during motor neuron differentiation. Mitochondrial biogenesis is the process by which cells increase their mitochondrial components and includes upstream mRNA signaling, mtDNA copy number and gene expression, electron transport chain protein expression, and mitochondrial mass. Although many of these processes are regulated by the same mechanisms, they may also act independently of each other, resulting in an increase of one without an increase in all of them. **Figure 10** depicts how mitochondrial biogenesis 'master regulator' PGC1-α increases transcription of genes encoding mitochondrial proteins as well as mitochondrial and non-mitochondrial sources of cellular ATP production.

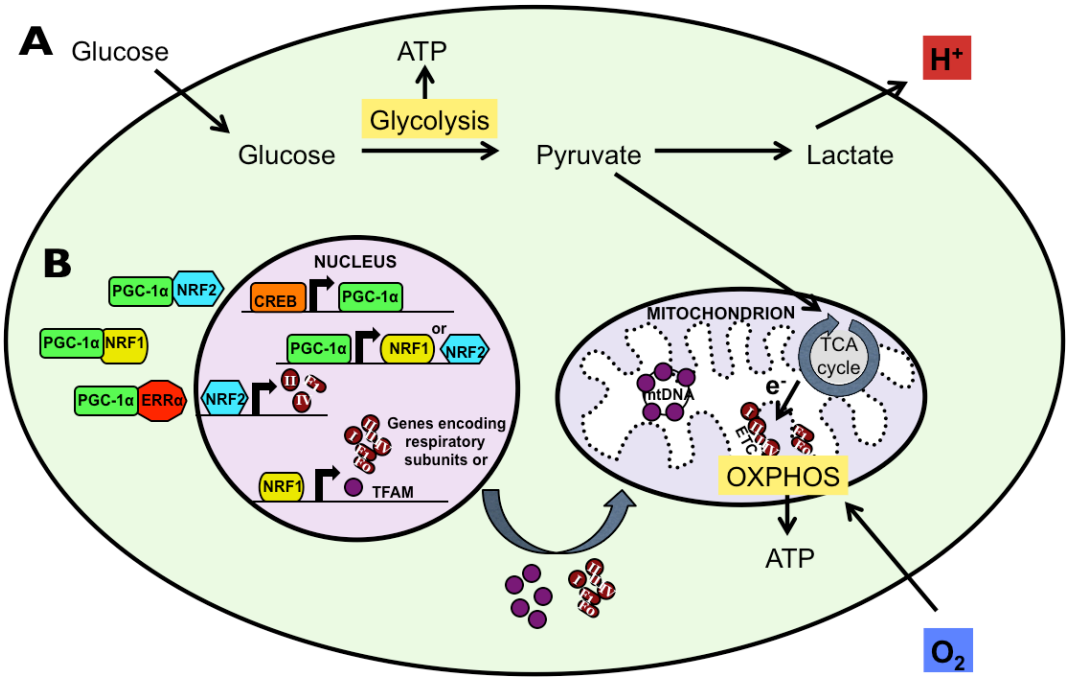


**Figure 10. Mitochondrial biogenesis and ATP production.** A) Anaerobic glycolysis is the process by which glucose is converted to pyruvate. Pyruvate can be converted into lactate anaerobically or oxidatively decarboxylated by the TCA cycle to electrons ($e^-$) that reduce $NAD^+/FAD^+$ to NADH/FADH which are then oxidized by the electron transport chain (ETC) to generate ATP during oxidative phosphorylation (OXPHOS) B) Mitochondrial biogenesis regulator PGC-1α binds to NRF1/2 and ERRα, initiating gene expression of mitochondrial components.

## 4.2 Results

### 4.2.1 Mitobiogenesis signaling increases with motor neuron differentiation

In order to assess mitochondrial biogenesis as cells differentiate from hESC-derived hNSCs to motor neurons, qPCR targeting biogenesis genes was performed at seven-day time points. **Figures 11A and B** shows increased levels of PGC-1α at D21, POLG at D28, and ERRα, NRF1 and POLRMT at D21 and D28 compared to D0 (n=4-6, $p<0.01$, one-way ANOVA, *$p<0.05$, **$p<0.01$, ***$p<0.001$, Dunnett's multiple comparisons test). NRF2, TFAM, and TFMB2 expression remained unchanged ($p<0.05$, one-way ANOVA). Based on these findings D21 was chosen as the time point for analysis of iPSC-derived cells. There was no change in PGC-1α, POLG, POLRMT, or TFAM expression but there was an increase in ERRα at D21 in iPSC-derived cells (**Figure 11C;** n=3, *$p<0.05$, unpaired t-test).

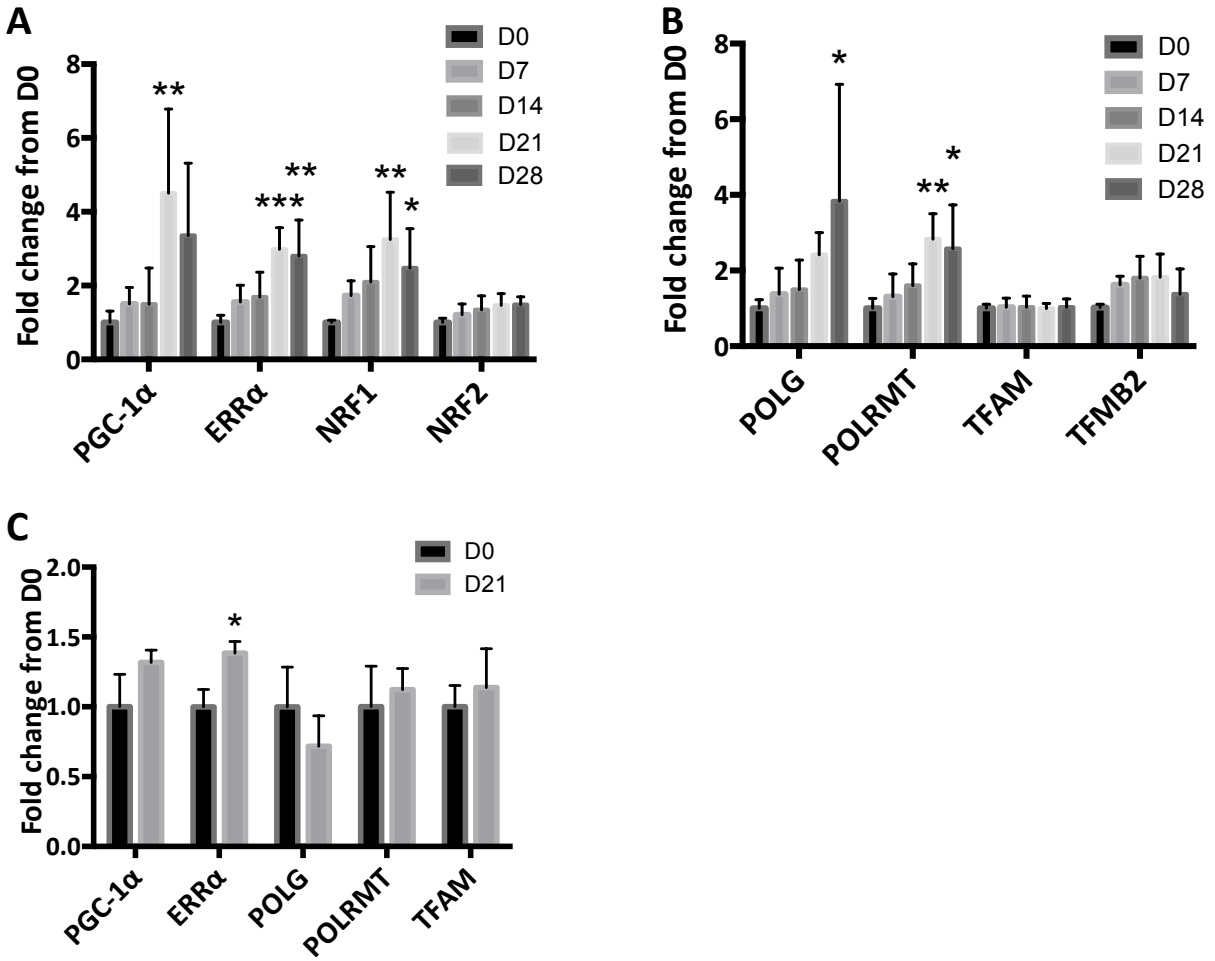


**Figure 11. Mitochondrial biogenesis signaling during motor neuron differentiation.** Expression of upstream (A) and downstream (B) mitochondrial biogenesis genes in hESC-derived cells at D0 (hNSCs) and on day 7-28 of motor neuron differentiation C) Expression of mitochondrial biogenesis genes in iPSC-derived cells at D0 (hNSCs) and D21 (motor neurons). *p<0.05, **p<0.01, ***p<0.001

4.2.2 Mitochondrial encoded genes increase with motor neuron differentiation.

The nuclear genome encodes most of the proteins that mitochondria require; however, mitochondria have their own genome that encodes 13 proteins essential for respiratory chain function. To determine if mitochondrial gene expression was increased during motor neuron differentiation we measured with qPCR expression of four mtDNA-encoded genes. **Figure 12A** shows an increase in ND2 and ND4 expression on D21 and D28 compared to D0 in hESC-derived cells (n=4-6, *p<0.05, one way ANOVA, *p<0.05, Dunnett's multiple comparisons test). However, there was no statistically significant increase in iPSC-derived cells on D21 compared to D0 because of variability in the D21 samples (**Figure 12B**, n=3, p>0.05, unpaired t-test).

qPCR was also performed with genomic DNA as the input. When analyzed using a standard curve of human mtDNA samples we were able to determine the mtDNA copy number. This analysis revealed a non-significant decrease in mtDNA copy number in hESC-derived cells (**Figure 12C**), as well as a significant decrease in mtDNA copy number in iPSC-derived cells with motor neuron differentiation (**Figure 12D;** *p<0.05). Because the four genes chosen are spatially distributed around the mitochondrial genome we are also able to detect mtDNA deletions using this method. Since there are no differences in the expression levels of the four genes at any time point we know that there are likely no major mtDNA deletions in those areas.

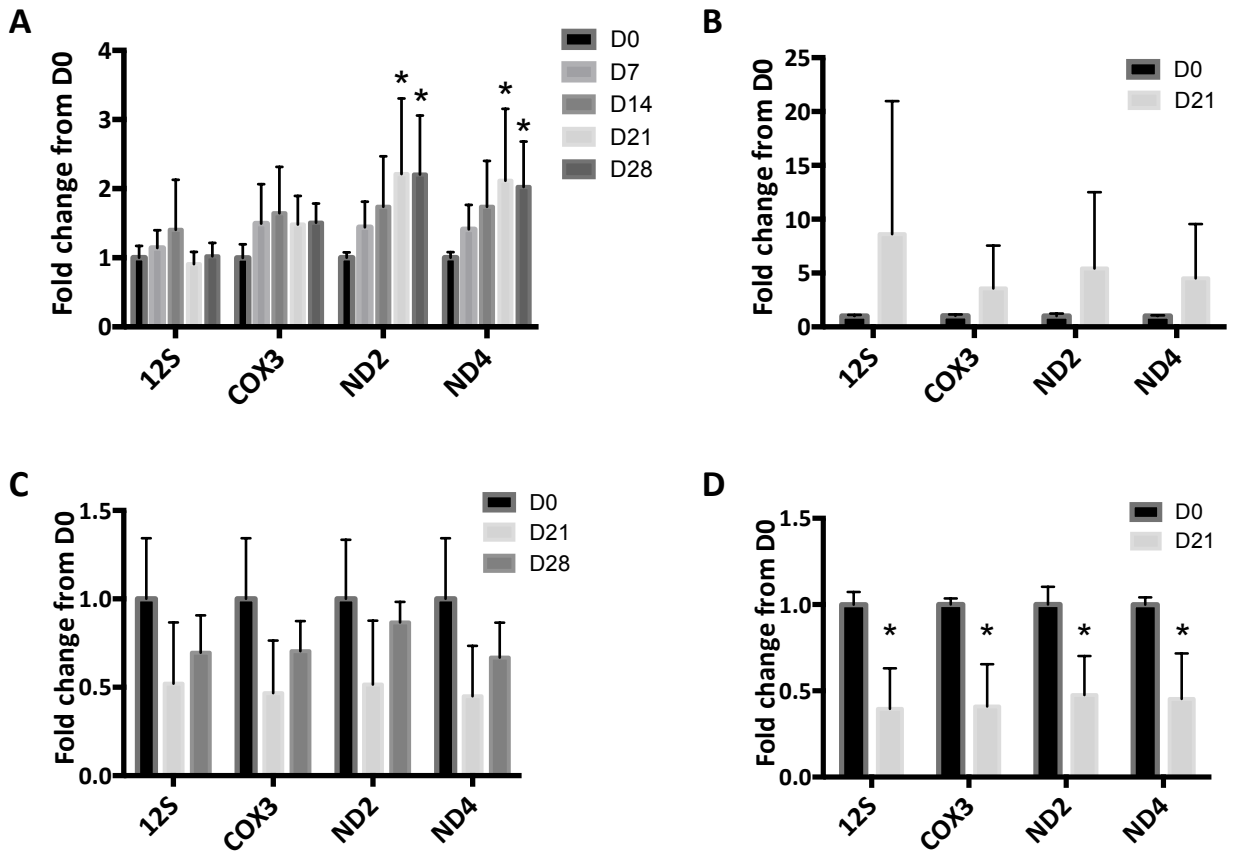


**Figure 12. Mitochondrial encoded gene expression and mtDNA copy number.** A) Expression of mitochondrial encoded genes in hESC-derived cells at D0 (hNSCs) and on day 7-28 of motor neuron differentiation B) Expression of mitochondrial encoded genes in iPSC-derived cells at D0 (hNSCs) and D21 (motor neurons) C) mtDNA copy number in hESC-derived cells, and D) iPSC-derived cells. *p<0.05

### 4.2.3 Glycolysis decreases as cells differentiate into motor neurons

For respiration analysis oxygen consumption rate (OCR) and extracellular acidification rate (ECAR) were measured simultaneously in adherent cultures using the XF24 Extracellular Flux Analyzer. This instrument allows measurement from 20 wells of cells plus 4 control wells. ECAR is measured in milli-pH units (mpH) and measures the change in pH resulting from the release of protons from the cell during glycolysis. In order for these readings to be accurate they must be within the linear range of the XF24 instrument. In order to determine optimal cell density three or four densities, ranging from 20,000 to 80,000 cells per well, were measured for each cell type. The iPSC cell line is denoted C42 here. **Figure 13** shows basal OCR and ECAR as a function of cell number. As seen with both hNSC lines (H9 D0 and C42 D0), 80,000 cells per well gives signals beyond the linear range of the XF24 instrument (**Figure 13A and C**). Based on these data as well as variability between wells (data not shown), we chose 40,000 cells per well for H9 D0 and 60,000 cells per well for H9 D21, C42 D0, and C42 D21.

In order to assess electron transport chain function, a number of inhibitors are commonly used including oligomycin, FCCP, rotenone, and antimycin A. Oligomycin is added to inhibit ATP synthase, followed by the protonophore FCCP to dissipate the proton gradient and measure maximal OCR in an uncoupled state, rotenone to inhibit complex I and antimycin A to inhibit complex III. Starting concentrations of these inhibitors were chosen based on published protocols [130, 137]. Interestingly, the starting concentration of 0.3 μM FCCP was insufficient to uncouple respiration in both hESC- and iPSC-derived cells. Since an excess of FCCP can uncouple the plasma membrane, it was important to determine the lowest concentration required to uncouple

mitochondrial respiration. 0.5-2 μM FCCP were tested in both cell types optimal concentration was chosen based on an increase from oligomycin inhibited levels (0.5 μM for hESC-derived and 1 μM for iPSC-derived). Interestingly, no concentration of FCCP increased OCR above basal levels in either cell type. This suggests that cells are respiring at maximum capacity.

**Figure 14A** shows a representative recording of iPSC-derived cells on D0 (green) and D21 (blue). Temperature control wells are shown in teal. Dotted lines represent an average of the three time points. Respiration analysis was performed on hESC- (**Figure 14B**) and iPSC-derived cells (**Figure 14C**). There was no change in basal respiration or after addition of any of the inhibitors on D21 compared to D0 in either cell type ($p>0.05$, unpaired t-test). We did not detect changes in oxygen consumption coupled to ATP synthesis or max respiratory capacity in either cell type.

ECAR was measured simultaneously in these cultures. There was a significant decrease in ECAR at D21 compared to D0 in both hESC-derived cultures (**Figure 15A**), as well as iPSC-derived cultures (**Figure 15B; ***$p<0.05$). This suggests a decreased usage of glycolysis in motor neurons compared to hNSCs.

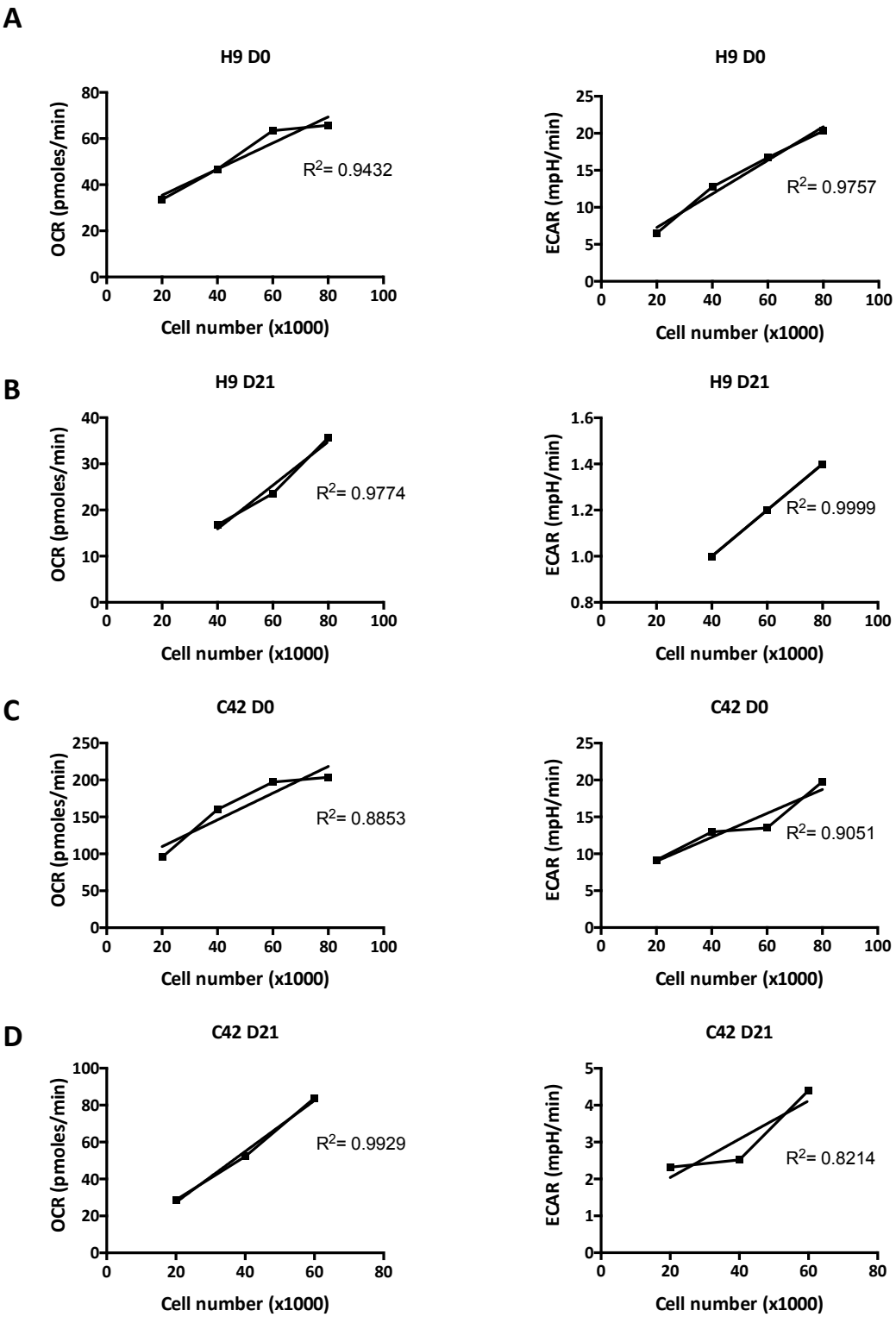


**Figure 13. OCR and ECAR values as a function of cell density** A) hESC-derived cells (H9) on D0 and B) D21 C) iPSC-derived cells (C42) on D0 and D) D21

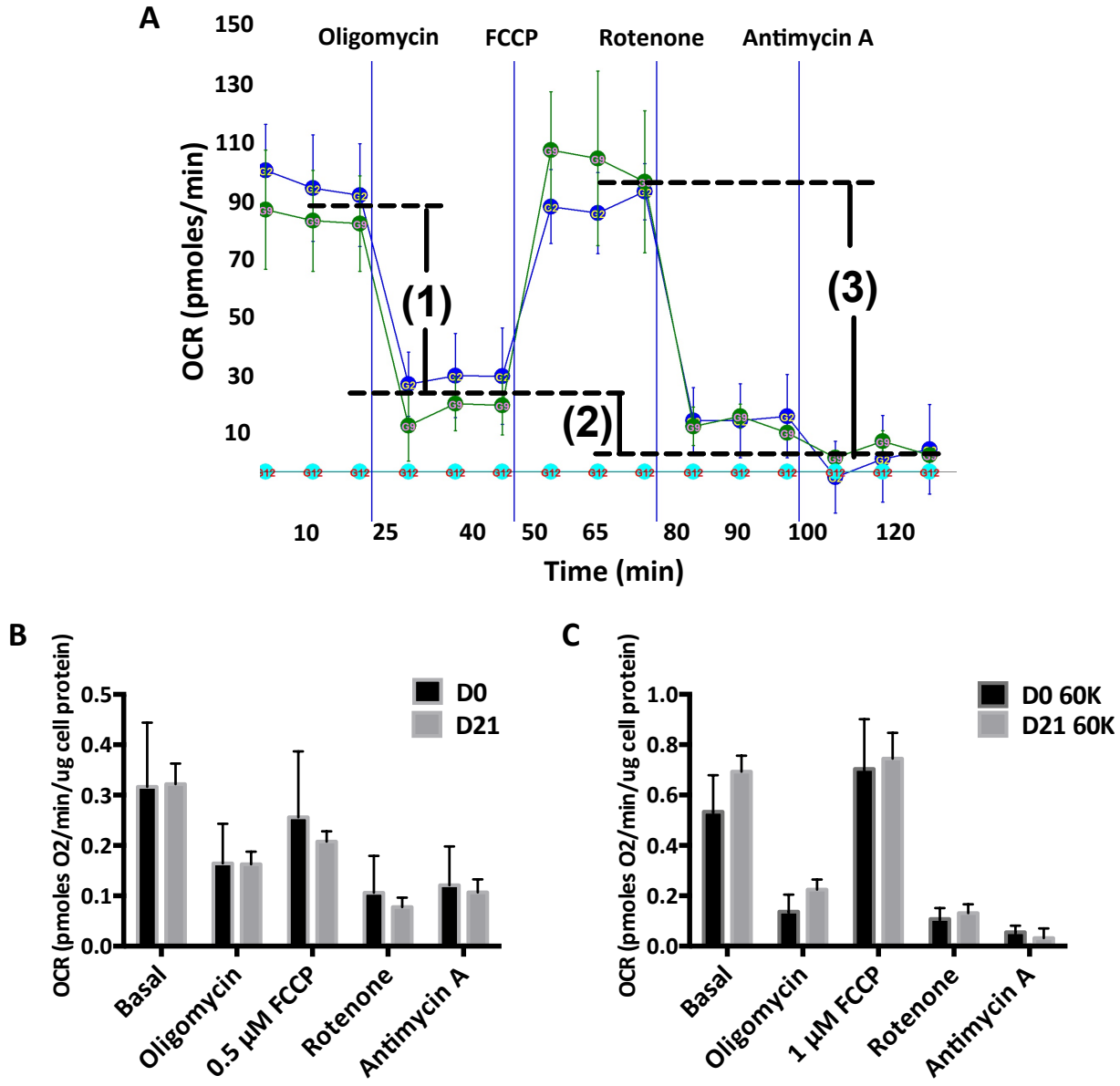


**Figure 14. Bioenergetic profile of hNSCs and motor neurons.** A) Representative measurements from iPSC-derived cells showing oxygen consumption rate (OCR) after the addition of various electron transport chain inhibitors. (1) represents OCR coupled to ATP synthesis, (2) is the amount of proton leak across the mitochondrial inner membrane, and (3) is max respiratory capacity B) OCR normalized to cell protein in hESC-derived cells C) iPSC-derived cells

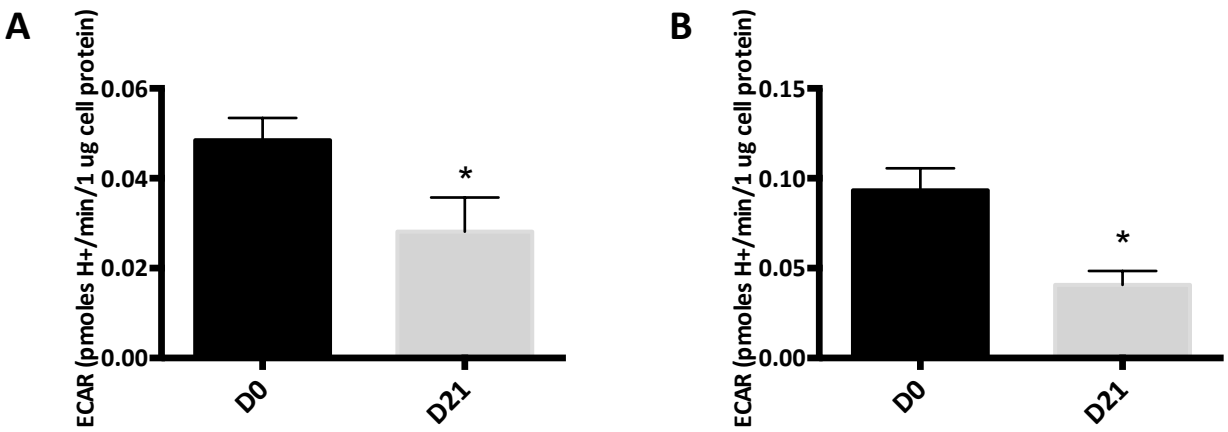


**Figure 15. ECAR in hNSCs and motor neurons.** Extracellular acidification rate (ECAR), a measure of glycolysis, normalized to cell protein in hESC-derived cells (A), and iPSC-derived cells (B). *p<0.05

4.2.4 Electron transport chain proteins, but not mitochondrial mass, increase with differentiation

To further investigate mitochondrial biogenesis as hNSCs differentiate into motor neurons we measured protein expression of electron transport chain proteins. As shown in **Figure 16B**, in hESC-derived cells, levels of complex II (CII) and complex V (CV) proteins were significantly increased on D21 and D28, respectively (n=3-4). All other proteins were increased at both time points but did not reach statistical significance. To increase statistical power, respiratory proteins normalized to their representative D0 were combined and this revealed a significant increase on D21 and D28 (**Figure 16C**). In iPSC-derived cells there was a significant increase in complex III (CIII) and complex V (CV) on D21 (n=4, **Figure 16E**). When combined, respiratory proteins were significantly increased on D21 (**Figure 16F**).

To measure mitochondrial mass protein expression of an outer mitochondrial membrane protein, voltage-dependent anion channel 1 (VDAC1), was analyzed. Interestingly, the VDAC1 protein levels were unchanged in hESC-derived cells on D21 and D28 (**Figure 17A**) and iPSC-derived cells on D21 compared to D0 (**Figure 17B**). To further confirm that mitochondrial mass is unchanged during motor neuron differentiation, hESC-derived cells were immunostained for the translocase of outer mitochondrial membrane, TOM20. Localization of mitochondria changed from perinuclear in hNSCs to extended into long processes on D21. However, when TOM20 fluorescence in 10 representative fields was normalized to cell number there was no difference in fluorescence between D0 and D21 (**Figure 17D**).

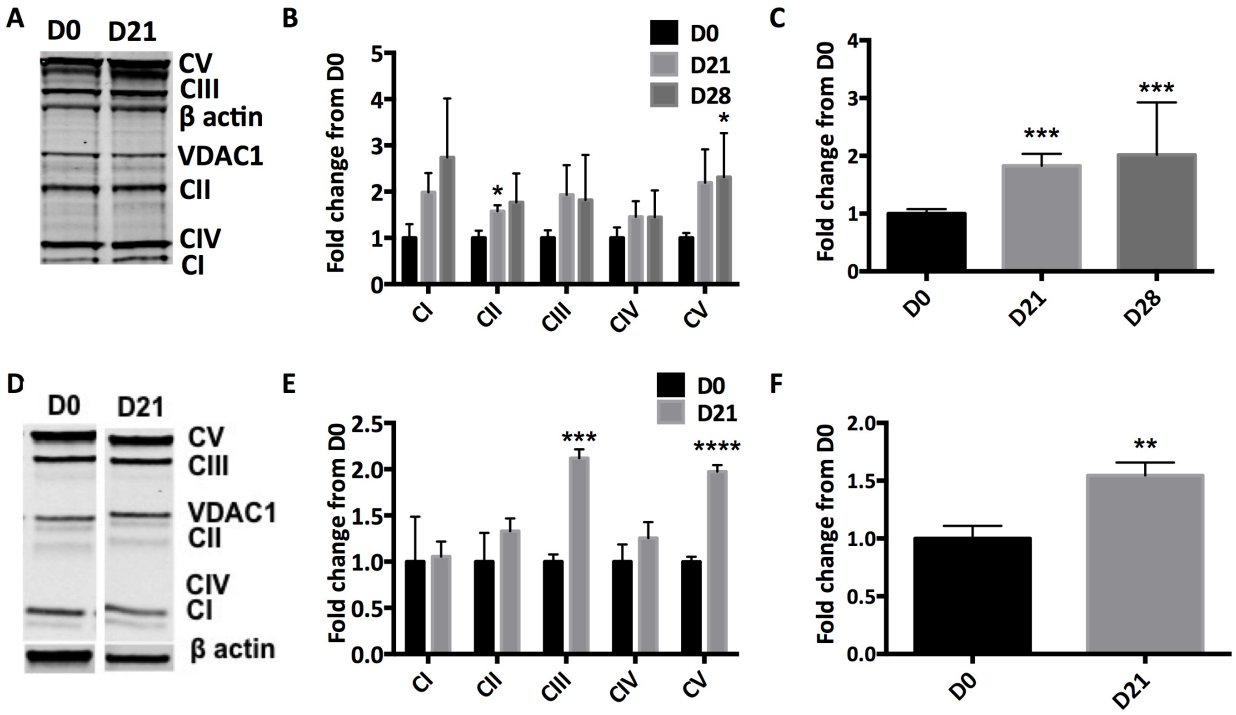


**Figure 16. Respiratory chain protein expression in hNSCs and motor neurons.** A) Representative western blot of hESC-derived cells B) Western blot quantitation normalized to beta actin C) Respiratory chain protein expression in hESC-derived cells D) Representative western blot of iPSC-derived cells E) Quantitation normalized to beta actin F) Respiratory chain protein expression in iPSC-derived cells. *p<0.05, **p<0.01, ***p<0.001

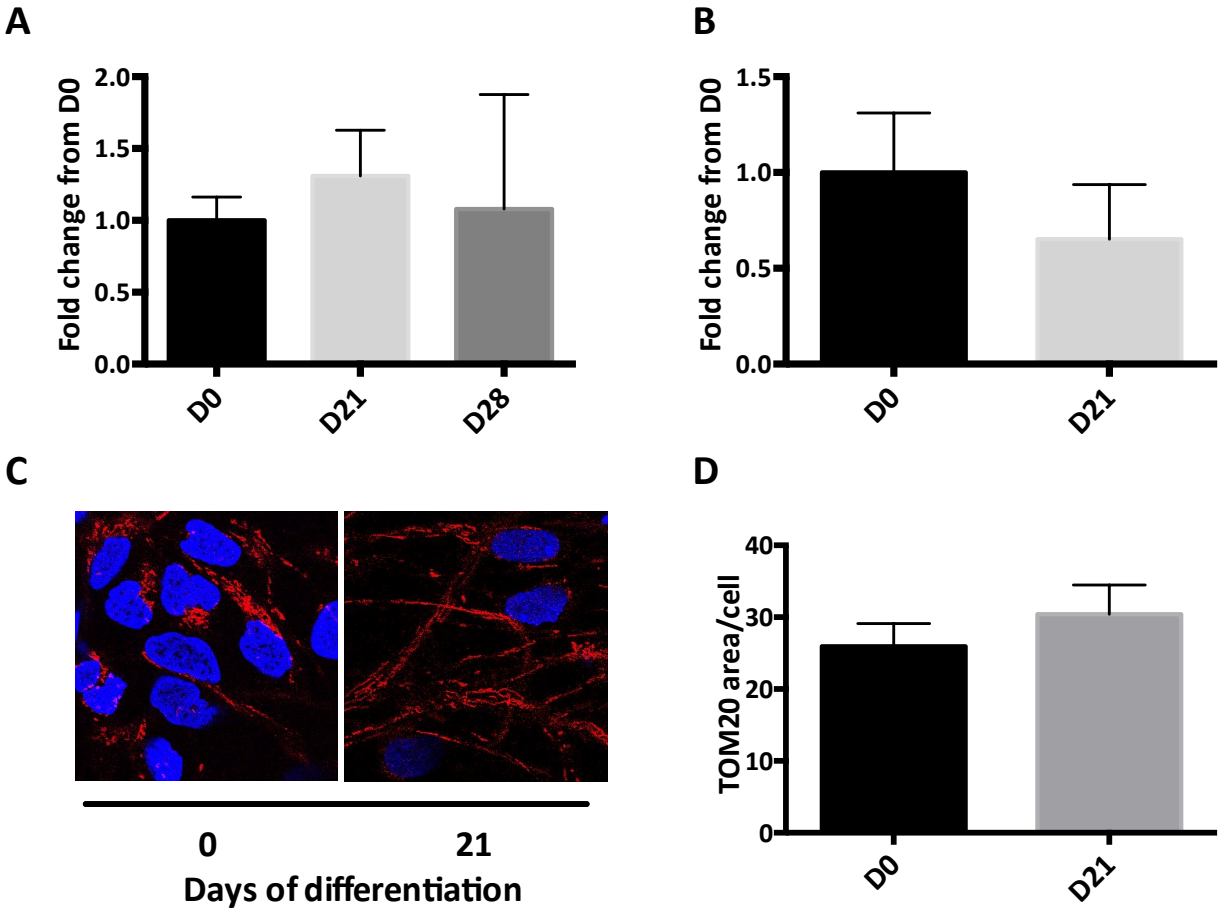


**Figure 17. Mitochondrial mass in hNSCs and motor neurons.** A) VDAC1 protein expression in hESC-derived cells normalized to beta actin B) VDAC1 protein expression in iPSC-derived cells normalized to beta actin C) Representative image of TOM20 staining in hESC-derived cells E) Quantitation of TOM20 staining in hESC-derived cells

## 4.3 Summary

In summary, this series of experiments demonstrated that mitochondrial biogenesis signaling and electron transport chain protein expression increases during motor neuron differentiation of hNSCs. This is not accompanied by an increase in mtDNA copy number or mitochondrial mass, suggesting that the total amount of mitochondria in the cell is not changing. Although there is no change in respiration rates there is a significant decrease in glycolysis between hNSCs and motor neurons. Together, these results indicate that mitochondrial biogenesis is increased during motor neuron differentiation and is accompanied by a reduction in glycolysis.

# CHAPTER FIVE

## Electrophysiological changes as cells differentiate into motor neurons

### 5.1 Rationale and Hypothesis

Development of voltage-activated currents and the generation of action potentials are crucial to motor neuron maturation *in vivo*. In order to explore these properties *in vitro* we performed whole cell patch clamp on hESC- and iPSC-derived motor neurons. We expected that after four weeks of motor neuron differentiation cells would display currents characteristic of excitable cells and generate action potentials following depolarizing current injection. These findings will set the stage for further analysis of voltage gated ion channels underlying motor neuron excitability in healthy and disease states.

### 5.2 Results

#### 5.2.1 Identifying motor neurons in live culture

In order to identify motor neurons in live cultures a lentivirus was generated with GFP under control of a motor neuron specific transcription factor (HB9). To increase the rate of viral infection, cells were treated with the cationic polymer protamine sulfate. This polymer was chosen over polybrene, a commonly used viral infection enhancer, because this latter agent was toxic to motor neurons used in this study. Optimal multiplicity of infection (MOI) and virus incubation time was determined for each cell type. Cells were infected with the lentivirus 5 days before recording and replated on glass coverslips 2 days before recording.

### 5.2.2 Passive membrane properties of hESC and iPSC-derived cells

Passive membrane properties were recorded after the whole cell patch clamp configuration was acquired and monitored over the course of the recording on day 28 of motor neuron differentiation. Membrane capacitance (Cm) was 14.88 ± 1.42 pF for hESC-derived cells (n=5) and 9.75 ± 0.45 pF for iPSC-derived cells (n=7; **Figure 18A**). Resting membrane potential (Vm) was -39 ± 3.84 mV (n=6) in hESC- and -31.6 ± 4.82 mV (n=10) in iPSC-derived cells (**Figure 18B**). Membrane resistance (Rm) was 2±0.3 GΩ in hESC-derived cells (n=5) and 3.77±0.85 GΩ in iPSC-derived cells (n=6; **Figure 18C**). None of these parameters were statistically different between cell types.

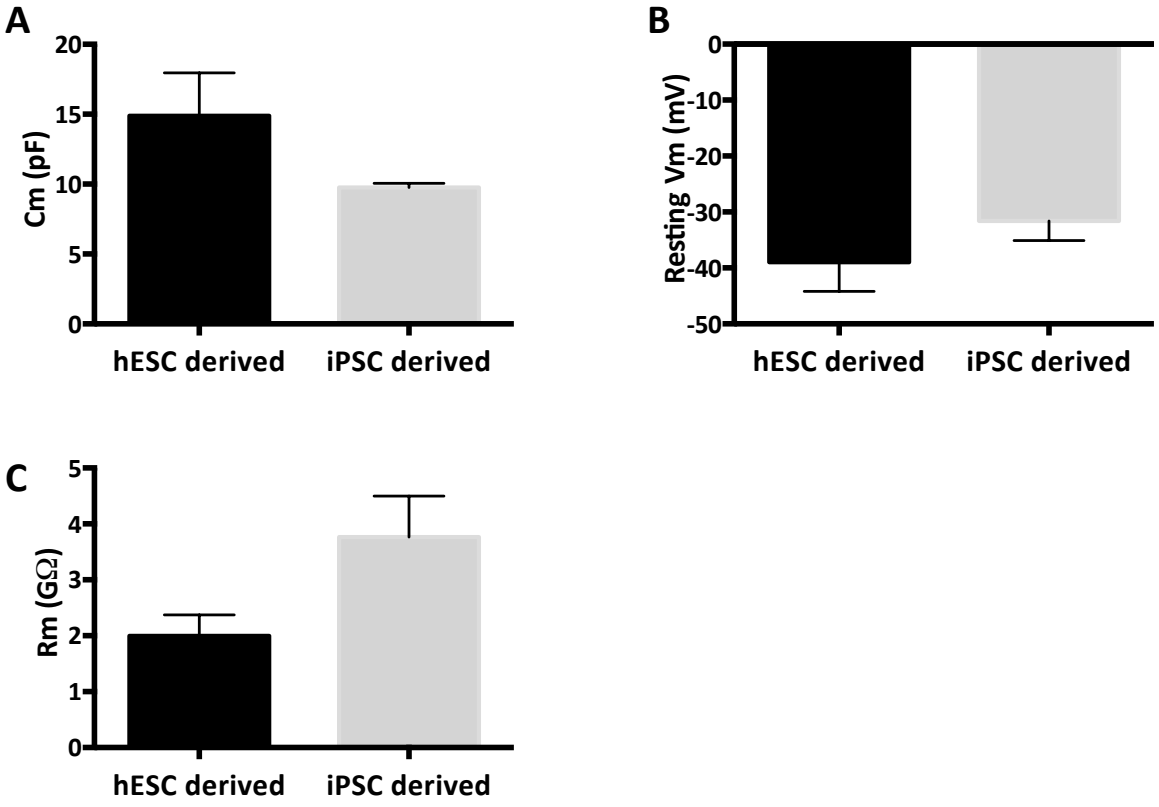


**Figure 18. Passive membrane properties in hNSC-derived motor neurons.** A) Membrane capacitance (Cm), B) Resting membrane potential (Vm), and C) Membrane resistance (Rm) in hESC- and iPSC-derived motor neurons.

5.2.3 Voltage gated currents characteristic of excitable cells

A series of voltage steps from a holding potential for -60 revealed inward and outward currents characteristic of sodium and potassium currents, respectively. **Figure 19A (i)** shows a representative recording from an iPSC-derived motor neuron on D28. The presence of sodium channels was confirmed by the addition of 2 μM tetrodotoxin (TTX, **Figure 19A (ii)**). In order to determine current densities normalized to cell size, peak current amplitude was divided by cell capacitance. Mean sodium current density was -29.10 ± 8.29 pA/pF (n=5) for hESC-derived cells and -37.51 ± 5.39 pA/pF (n=7) for iPSC-derived cells (**Figure 19B**). Mean potassium current density was 29.55 ± 9.25 pA/pF (n=5) for hESC-derived cells and 78.91 ± 8.04 pA/pF (n=7) for iPSC-derived cells (**Figure 19C**). Interestingly, iPSC-derived motor neurons had a significantly higher potassium channel density than hESC-derived cells.

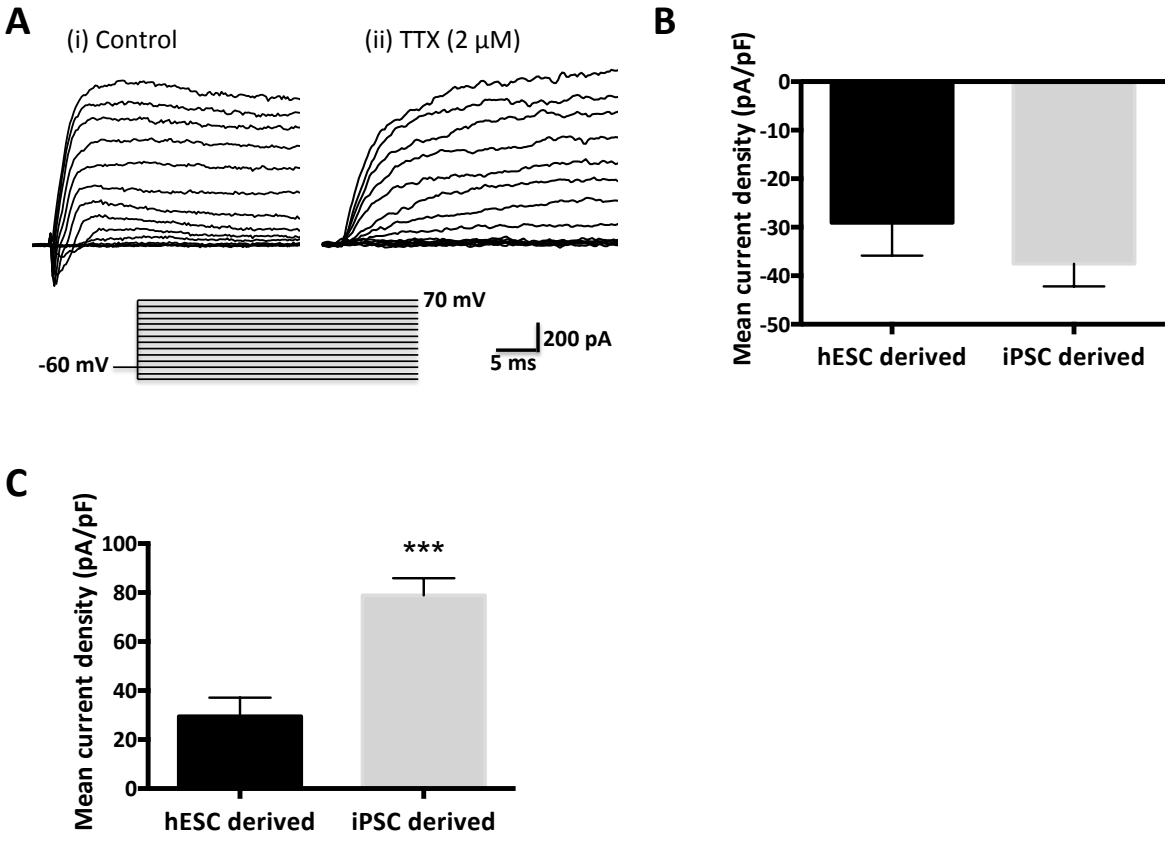


**Figure 19. Voltage gated currents in hNSC-derived motor neurons.** A) (i) A representative voltage clamp trace from an iPSC-derived motor neuron (ii) the same cell after the addition of 2 µM (TTX) to block voltage activated sodium channels. B) Mean sodium current density and C) Mean potassium current density in hESC- and iPSC-derived cells ***p<0.001

5.2.4 Action potential firing of stem cell derived motor neurons

Action potentials were elicited by a series of current pulses of increasing injected current amplitude under the current clamp mode of the patch clamp technique. Approximately 40% of hESC-derived cells and 60% of iPSC-derived cells fired action potentials on D28. A representative trace from a hESC-derived cell is shown in **Figure 20A**. After action potential generation was confirmed, the minimum amount of current injection necessary to generate an action potential, rheobase, was determined by increasing the current injection by 0.01 nA. Rheobase was 23.75 ± 9.44 pA in hESC-derived motor neurons (n=4) and -10.75 ± 11.88 pA in iPSC-derived motor neurons (n=4; $p>0.05$; **Figure 20B**). The fact that some iPSC-derived cells fire action potentials after hyperpolarizing current injection suggests the ability for spontaneous action potential formation. The threshold potential for the upstroke of the action potential and action potential height was similar for both cell types (**Figure 20B**).

A

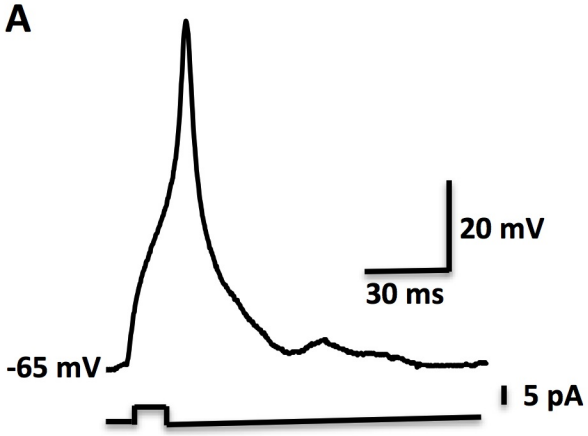


B

| | Vm (mV) | Rheobase (pA) | AP threshold (mV) | AP height (mV) |
|---|---|---|---|---|
| **hESC-derived** | -39.0 ± 3.84 | 23.75 ± 9.44 | 22.66 ± 7.48 | -41.73 ± 10.14 |
| **iPSC-derived** | -31.6 ± 4.82 | -10.75 ± 11.88 | 24.72 ± 4.18 | -41.12 ± 5.02 |

**Figure 20. Action potential generation in hNSC-derived motor neurons.** A) A representative current-clamp recording showing action potential formation in a hESC-derived motor neuron B) The resting membrane potential (Vm), minimum current injection required to fire an action potential (rheobase), action potential (AP) threshold, and AP height for both cell types

## 5.3 Summary

Taken together, these preliminary results provide evidence that cells develop voltage gated channels characteristic of excitable cells and are able to generate action potentials on D28 of motor neuron differentiation. Similar effects were seen in hESC- and iPSC-derived cells. Combined with mRNA and protein analysis, these findings suggest that hNSC-derived cells are developing into functional motor neurons. These studies set the stage for future analysis of stem cell derived motor neurons including the alteration of excitability by pharmacological means.

# CHAPTER SIX: DISCUSSION

## 6.1 Generation of motor neurons from hNSCs

The goal for the first set of studies was to generate motor neurons from hNSCs. In order to develop a protocol for patient cell use we reprogrammed PBMCs into iPSCs. Following neural induction 67% of these cells stained positive for the hNSC marker nestin. These cells, as well as commercially available hESC-derived hNSCs (>90% nestin positive) were further differentiated into motor neurons. After 21 days of motor neuron differentiation cells had significantly increased expression of genes normally found in motor neurons including the motor neuron specific transcription factor HB9. ~45% of hESC- and ~10% of iPSC-derived cells co-stained positive for markers of post-mitotic spinal motor neurons and a more general neuronal marker. The findings in hESC-derived cells were consistent with a previous study using a similar protocol which reported ~30% motor neurons, but iPSCs showed a much lower rate of motor neuron generation. These results demonstrate for the first time that iPSCs derived from PBMCs can differentiate into motor neurons.

There was a higher percentage of motor neurons in hESC- compared to iPSC-derived cultures (~45% vs ~10%, respectively). This may be due to more efficient neural induction since hESCs were >90% nestin positive compared to 67% in iPSC-derived cells. This could be also be due to changes in the protocol including a shortened embryoid body stage and only four days of dual SMAD inhibition compared to seven in the previous study [128].

Motor neurons derived from hPSCs give us the ability to study a cell type previously only accessible in post mortem tissue. However, the artificial environment in which they are grown has limitations. We have shown that retinoic acid (RA) and purmorphamine (PM) exposure is sufficient to induce motor neuron differentiation in hESC-derived cells but there are a number of other signaling molecules present in the developing embryo that were not added *in vitro*. In order to more closely replicate physiological conditions for the iPSC-derived motor neuron differentiation protocol, we added small molecules to inhibit SMAD signaling and BDNF during early differentiation and GDNF/CNTF for trophic support after day 14. Previous studies have shown that SMAD inhibition efficiently neutralizes hNSCs [138, 139]. Another artificial aspect of this culture environment is that it does not allow motor neurons to interact with other cell types including glia. The lack of GFAP staining is consistent with a previous study using a similar protocol [128] and suggests that there are no astrocytes, but we did not perform oligodendrocyte staining. Furthermore, these motor neurons do not form functional synapses with muscle, their *in vivo* targets. Previous studies have shown the ability of hESC- and iPSC-derived motor neurons to make functional synapses on muscle cells in culture but we do not yet know how this affects motor neuron maturation and firing. Finally, traditional cell culture grows cells in a single layer, compared to the three dimensional nature of tissue. There has been recent interest in developing three-dimensional cell culture systems but much work remains if this is to be a feasible model for more than a few select labs (for a review see [140]. A three-dimensional culture system would provide the spatial organization of tissue, in addition to allowing more accurate gradient signaling important during development.

PBMCs were chosen as starting material for reprogramming over fibroblasts, which are more commonly used. Collecting peripheral blood is a much simpler and less invasive procedure than a skin punch for fibroblast collection. Since these cells are not exposed to environmental mutagens they may be clinically more favorable due to less DNA mutations. Furthermore, PBMCs have a DNA methylation profile that more closely resembles hESCs [89], suggesting that they may reprogram more easily. Indeed, a previous study found that PBMCs could be reprogrammed with greater efficiency and two weeks faster than fibroblasts [89]. PBMCs may also more accurately replicate disease pathology. The current study showed that PBMCs from sALS patients had less mtDNA encoded genes compared to control patients [26]. This replicates what is seen in post mortem spinal cord of ALS patients [26]. Blood cells are unaffected in ALS and this decrease in mitochondrial gene expression may represent a systemic bioenergetic impairment that has not been previously characterized. If motor neurons derived from these cells share the same decreased expression they may be a useful model of sALS. Furthermore, if mtDNA gene expression is consistently decreased in all ALS patients this panel of genes may be used as a biomarker for ALS.

## 6.2 Mitobiogenesis signaling in hPSC-derived motor neurons

The goal for this series of experiments was to investigate mitochondrial biogenesis during motor neuron differentiation. Gene expression of mitochondrial biogenesis ‘master regulator’ PGC-1α and many of its downstream targets were increased in hESC-derived cells during differentiation and expression peaked on day 21. This is consistent with PGC-1α activating ERRα and NRF1 to increase transcription

of downstream POLG and POLRMT. Expression of mitochondrial transcription factors TFAM and TFMB2 was unchanged, consistent with no significant change in mtDNA copy number in these cells. iPSC-derived cells increased expression of ERRα on day 21. The finding that not all mitobiogenesis genes were increased could mean that these cells increase mitobiogenesis gene expression earlier or later in the differentiation process, given that only one time point was analyzed in these cells. Expression of two mtDNA-encoded genes, ND2 and ND4, was also increased in hESC-derived cells on D21. However, there was too much variation in iPSC-derived samples to determine a statistically significant increase. In contrast, mtDNA copy number was decreased slightly in hESC- and significantly decreased in iPSC- derived motor neurons.

Respiration analysis revealed no change in basal respiration between hNSCs and motor neurons, but there was a decrease in glycolysis. One limitation of this series of studies is that cells were grown and differentiated in 5% oxygen but respiration analysis was performed in room air (~20% oxygen). Efforts were made to keep D0 and D21 cells in as similar conditions as possible (similar passage number, similar time in culture, etc.) but the change in oxygen concentration may have affected the cells. Interestingly, neither D0 nor D21 cells increased OCR levels above basal after the addition of FCCP. FCCP uncouples the proton gradient across the inner mitochondrial membrane, measuring maximum oxygen consumption. The fact that this value never exceeds basal levels suggests that the ETC is already running at maximum capacity in both cell types.

Although a decrease in glycolysis may result in increased OXPHOS, it doesn't necessarily mean there is an increase in mitochondrial mass. Mitochondrial mass could

remain the same but there could be more ETC complexes or they could be more efficient in OXPHOS. Indeed, we found an increase in respiratory proteins but no increase in mitochondrial mass. The proteins increased included complex II and V in hESC-derived cells and complex III and V in iPSC-derived motor neurons compared to hNSCs. One limitation of measuring ETC proteins this way is that each complex is composed of many proteins and we only analyzed one for each complex. Additionally, we are measuring protein expression; this does not ensure that proteins are assembled correctly and that the complex is functioning properly.

Similarly, an increase in ETC protein expression does not necessarily mean an increase in respiration. Respiration is a tightly controlled process. Potential ATP production and oxygen consumption capacity could be much greater than what is measured at basal levels. The observed increase in ETC protein expression may represent potential functioning of the ETC chain. For example, after strenuous exercise oxygen consumption and ATP production could be three times what it was at rest without any increase in mitochondrial mass. Uncoupling the proton gradient with FCCP showed maximal oxygen consumption but says nothing about ATP synthesis. Future studies to investigate this may compare ATP generation between hNSCs and motor neurons.

In summary, this series of studies suggest that some, but not all, mitobiogenesis processes increase with motor neuron differentiation of hNSCs. There may be differences in the timing of gene expression hESC- vs. iPSC-derived cells but it appears that both cell types decrease glycolysis and increase ETC protein expression without a change in mitochondrial mass during motor neuron differentiation. One process that the

current studies do not address is mitochondrial autophagy (mitophagy). Mitophagy is the cellular process that degrades dysfunctional mitochondria. This process could play a crucial role in the differentiation process and future studies could explore this.

## 6.3 Electrical maturation of hPSC-derived motor neurons

The aim of the last series of studies was to investigate the change in electrical properties of cells as they differentiated into motor neurons. Capacitance (Cm) was substantially lower in hNSC motor neurons (14.88 ± 1.42 pF in hESC-derived and 9.75 ± 0.45 pF in iPSC-derived) than rat spinal motor neurons at days 15-16 of gestation (E15-16; birth is E21-22; Cm = 29.3 ± 1.0 pF) [39]. Similarly, resting membrane potential was more depolarized (-39 ± 3.84 mV in hESC-derived and -31.6 ± 4.82 in iPSC-derived) than in E16 rat motor neurons (-49.3 ± 5.9 mV) [38]. Since Cm increases and Vm decreases with motor neuron maturation this may suggest that these cells are still very early in development and that later time points may reveal characteristics of more mature cells.

Similarly, sodium channel density was lower than what is seen in embryonic day 4 (E4) chick spinal motor neurons (-29.10 ± 8.29 pA/pF in hESC0-derived and -37.51 ± 5.39 pA/pF in iPSC-derived compared to ~70 pA/pF E4). Potassium channel density is lower in hESC-derived motor neurons (29.55 ± 9.25 pA/pF) than in embryonic day 4 (E4) chick spinal motor neurons (~65 pA/pF) but iPSC-derived motor neurons showed similar values (78.91 ± 8.04 pA/pF). Previous studies suggest that both current densities increase with motor neuron maturation so future studies may wish to investigate these properties in cells that were differentiated longer. There was a lot of variability in the

mean peak inward and outward currents, consistent with varying rates of maturation. Assessing later time points may also result in a greater similarity in maximal currents.

Action potentials were seen on D28 with threshold and rheobase values similar to a previous study [40]. The fact that some iPSC-derived cells fired action potentials in response to hyperpolarizing current injection is unusual and may be due to a number of factors, including rebound depolarization ($I_h$) that reached threshold. Future studies are planned to confirm this finding as well as to investigate repetitive action potential firing.

## 6.5 Use of hPSC-derived motor neurons for disease modeling

One potential use of patient iPSC-derived motor neurons is their use in modeling disease. If these cells replicate disease pathology they may be useful for testing promising drug compounds. Both hESC- and iPSC-derived motor neurons from this study have been used in preliminary studies to test molecules that mimic the neurotrophins, nerve growth factor (NGF) and brain-derived neurotrophic factor (BDNF). Neurotrophins promote neuronal growth and survival, but their structure does not allow them to pass the blood brain barrier (BBB) [141]. Dr. Achilleas Gravanis developed small molecules, called microneurotrophins, and three analogues were kindly provided for our studies. Unlike NGF and BDNF, microneurotrophins can pass the BBB. After hESC-derived motor neurons were treated with 100 nM of the three neurotrophin analogues, NGF, or vehicle control for four or 24 hours RNA was isolated and sent for microarray screening. Gene expression analysis was then performed to identify which of the three compounds activated pathways most similar to NGF. The BNN124 analogue most closely resembled NGF at both 4 and 24 hours. Based on these promising results,

we treated hESC- and iPSC-derived motor neurons with the three analogues, NGF, BDNF, or vehicle control for 24 hours and isolated RNA for RNA-sequencing (RNA-seq). RNA-seq data will be analyzed in the coming months and the findings will be published soon after. Both RNA-seq and microarray analyze gene expression; however, RNA-seq has a number of advantages. One advantage of RNA-seq is that it can detect very low expressing genes because it quantitates absolute rather than relative expression. Microarray technology is based on fluorescence and can only detect expression over baseline. Another advantage of RNA-seq is that it can detect novel isoforms and mutations because it does not require a known sequence like microarray does. Microneurotrophins have potential use in many neurodegenerative diseases including Alzheimer's disease, Parkinson's disease, and Huntington's disease, as well as in stroke and nerve injury (for a review see [142]).

## 6.7 Summary and conclusions

In summary, we have demonstrated the ability to differentiate motor neurons from both hESC- and iPSC- derived cells in three weeks. The hypothesis that differentiation of human pluripotent stem cells into electrically excitable motor neurons will result in increased mitochondrial biogenesis was confirmed at multiple levels. Expression of upstream regulatory genes increased, along with increased transcription of mtDNA-encoded genes, and increased levels of representative ETC proteins. Despite these increases, mitochondrial mass remains unchanged. During this time cells develop voltage-gated currents characteristic of excitable cells and are able to fire action potentials in response to depolarizing current.

## 6.8 Significance and perspectives

The findings from this study have implications in multiple areas. Motor neurons are lost in a number of other diseases including progressive bulbar palsy, pseudobulbar palsy, primary lateral sclerosis, progressive muscular atrophy, and spinal muscular atrophy. Being able to generate motor neurons from patient blood cells may aid in the development of treatments for these devastating diseases by better understanding disease mechanisms and having predictive models to test promising compounds. The current study also sets the stage for looking at mitobiogenesis in other cell types lost in neurodegenerative disease including Parkinson's and Alzheimer's disease. Since mitochondrial dysfunction is a common theme in many neurodegenerative diseases a better understanding of how this pathway is regulated may lead to more effective drug targets. The findings in the present study suggest that PGC-1α acts through a NRF1-ERRα mediated pathway to increase mitobiogenesis in hESC-derived cells and this may represent a target to increase mitobiogenesis. Together, findings from this study provide the first evidence that iPSCs from blood can differentiate into electrically active motor neurons and that mitobiogenesis is increased during motor neuron differentiation in both hESC- and iPSC-derived cells. Future studies are planned to investigate the effects of microneurotrophins and SK channel activators on the electrical excitability of these stem cell derived motor neurons.

## REFERENCES


1. Borthwick GM, Johnson MA, Ince PG, Shaw PJ, Turnbull DM. Mitochondrial enzyme activity in amyotrophic lateral sclerosis: implications for the role of mitochondria in neuronal cell death. **Ann Neurol**. 1999;46:787-790.
2. Wiedemann FR, Manfredi G, Mawrin C, Beal MF, Schon EA. Mitochondrial DNA and respiratory chain function in spinal cords of ALS patients. **J Neurochem**. 2002;80:616-625.
3. Keeney PM, Bennett JP, Jr. ALS spinal neurons show varied and reduced mtDNA gene copy numbers and increased mtDNA gene deletions. **Mol Neurodegener**. 2010;5:21.
4. Vielhaber S, Kunz D, Winkler K, Wiedemann FR, Kirches E, Feistner H, Heinze HJ, Elger CE, Schubert W, Kunz WS. Mitochondrial DNA abnormalities in skeletal muscle of patients with sporadic amyotrophic lateral sclerosis. **Brain**. 2000;123 ( Pt 7):1339-1348.
5. Thau N, Knippenberg S, Korner S, Rath KJ, Dengler R, Petri S. Decreased mRNA expression of PGC-1alpha and PGC-1alpha-regulated factors in the SOD1G93A ALS mouse model and in human sporadic ALS. **J Neuropathol Exp Neurol**. 2012;71:1064-1074.
6. Wallace DC. Mitochondrial diseases in man and mouse. **Science**. 1999;283:1482-1488.
7. Taanman JW. The mitochondrial genome: structure, transcription, translation and replication. **Biochimica et biophysica acta**. 1999;1410:103-123.
8. Corral-Debrinski M, Horton T, Lott MT, Shoffner JM, Beal MF, Wallace DC. Mitochondrial DNA deletions in human brain: regional variability and increase with advanced age. **Nature genetics**. 1992;2:324-329.
9. Kraytsberg Y, Kudryavtseva E, McKee AC, Geula C, Kowall NW, Khrapko K. Mitochondrial DNA deletions are abundant and cause functional impairment in aged human substantia nigra neurons. **Nature genetics**. 2006;38:518-520.
10. Bender A, Krishnan KJ, Morris CM, Taylor GA, Reeve AK, Perry RH, Jaros E, Hersheson JS, Betts J, Klopstock T, Taylor RW, Turnbull DM. High levels of mitochondrial DNA deletions in substantia nigra neurons in aging and Parkinson disease. **Nature genetics**. 2006;38:515-517.
11. Onyango IG, Lu J, Rodova M, Lezi E, Crafter AB, Swerdlow RH. Regulation of neuron mitochondrial biogenesis and relevance to brain health. **Biochimica et biophysica acta**. 2010;1802:228-234.
12. Scarpulla RC. Metabolic control of mitochondrial biogenesis through the PGC-1 family regulatory network. **Biochim Biophys Acta**. 2011;1813:1269-1278.
13. Scarpulla RC, Vega RB, Kelly DP. Transcriptional integration of mitochondrial biogenesis. **Trends in endocrinology and metabolism: TEM**. 2012;23:459-466.
14. Martin E, Betuing S, Pages C, Cambon K, Auregan G, Deglon N, Roze E, Caboche J. Mitogen- and stress-activated protein kinase 1-induced neuroprotection in Huntington's disease: role on chromatin remodeling at the PGC-1-alpha promoter. **Hum Mol Genet**. 2011;20:2422-2434.
15. Lin JD. Minireview: the PGC-1 coactivator networks: chromatin-remodeling and mitochondrial energy metabolism. **Mol Endocrinol**. 2009;23:2-10.
16. Fernandez-Marcos PJ, Auwerx J. Regulation of PGC-1alpha, a nodal regulator of mitochondrial biogenesis. **Am J Clin Nutr**. 2011;93:884S-890.

17. Goffart S, Wiesner RJ. Regulation and co-ordination of nuclear gene expression during mitochondrial biogenesis. **Experimental physiology**. 2003;88:33-40.
18. Schreiber SN, Emter R, Hock MB, Knutti D, Cardenas J, Podvinec M, Oakeley EJ, Kralli A. The estrogen-related receptor alpha (ERRalpha) functions in PPARgamma coactivator 1alpha (PGC-1alpha)-induced mitochondrial biogenesis. **Proceedings of the National Academy of Sciences of the United States of America**. 2004;101:6472-6477.
19. Lin J, Handschin C, Spiegelman BM. Metabolic control through the PGC-1 family of transcription coactivators. **Cell metabolism**. 2005;1:361-370.
20. Mootha VK, Handschin C, Arlow D, Xie X, St Pierre J, Sihag S, Yang W, Altshuler D, Puigserver P, Patterson N, Willy PJ, Schulman IG, Heyman RA, Lander ES, Spiegelman BM. Erralpha and Gabpa/b specify PGC-1alpha-dependent oxidative phosphorylation gene expression that is altered in diabetic muscle. **Proceedings of the National Academy of Sciences of the United States of America**. 2004;101:6570-6575.
21. Fisher RP, Clayton DA. Purification and characterization of human mitochondrial transcription factor 1. **Molecular and cellular biology**. 1988;8:3496-3509.
22. Bonawitz ND, Clayton DA, Shadel GS. Initiation and beyond: multiple functions of the human mitochondrial transcription machinery. **Molecular cell**. 2006;24:813-825.
23. Boillee S, Vande Velde C, Cleveland DW. ALS: a disease of motor neurons and their nonneuronal neighbors. **Neuron**. 2006;52:39-59.
24. Robberecht W, Philips T. The changing scene of amyotrophic lateral sclerosis. **Nat Rev Neurosci**. 2013;14:248-264.
25. Gordon PH. Amyotrophic Lateral Sclerosis: An update for 2013 Clinical Features, Pathophysiology, Management and Therapeutic Trials. **Aging and disease**. 2013;4:295-310.
26. Ladd AC, Keeney PM, Govind MM, Bennett JP, Jr. Mitochondrial Oxidative Phosphorylation Transcriptome Alterations in Human Amyotrophic Lateral Sclerosis Spinal Cord and Blood. **Neuromolecular Med**. 2014.
27. Brockington A, Ning K, Heath PR, Wood E, Kirby J, Fusi N, Lawrence N, Wharton SB, Ince PG, Shaw PJ. Unravelling the enigma of selective vulnerability in neurodegeneration: motor neurons resistant to degeneration in ALS show distinct gene expression characteristics and decreased susceptibility to excitotoxicity. **Acta neuropathologica**. 2013;125:95-109.
28. DeJesus-Hernandez M, Mackenzie IR, Boeve BF, Boxer AL, Baker M, Rutherford NJ, Nicholson AM, Finch NA, Flynn H, Adamson J, Kouri N, Wojtas A, Sengdy P, Hsiung GY, Karydas A, Seeley WW, Josephs KA, Coppola G, Geschwind DH, Wszolek ZK, Feldman H, Knopman DS, Petersen RC, Miller BL, Dickson DW, Boylan KB, Graff-Radford NR, Rademakers R. Expanded GGGGCC hexanucleotide repeat in noncoding region of C9ORF72 causes chromosome 9p-linked FTD and ALS. **Neuron**. 2011;72:245-256.
29. Miller RG, Mitchell JD, Moore DH. Riluzole for amyotrophic lateral sclerosis (ALS)/motor neuron disease (MND). **The Cochrane database of systematic reviews**. 2012;3:CD001447.
30. Jessell TM. Neuronal specification in the spinal cord: inductive signals and transcriptional codes. **Nature reviews Genetics**. 2000;1:20-29.
31. Davis-Dusenbery BN, Williams LA, Klim JR, Eggan K. How to make spinal motor neurons. **Development**. 2014;141:491-501.

32. Spemann HM, H. Über induktion von Embryonalagen durch Implantation Artfremder Organisatoren. **Roux' Arch Entw Mech**. 1924:599-638.
33. De Robertis EM. Spemann's organizer and self-regulation in amphibian embryos. **Nature reviews Molecular cell biology**. 2006;7:296-302.
34. Maden M. Retinoic acid in the development, regeneration and maintenance of the nervous system. **Nature reviews Neuroscience**. 2007;8:755-765.
35. Pituello F. Neuronal specification: generating diversity in the spinal cord. **Current biology : CB**. 1997;7:R701-704.
36. Tanabe Y, William C, Jessell TM. Specification of motor neuron identity by the MNR2 homeodomain protein. **Cell**. 1998;95:67-80.
37. Carrascal L, Nieto-Gonzalez JL, Cameron WE, Torres B, Nunez-Abades PA. Changes during the postnatal development in physiological and anatomical characteristics of rat motoneurons studied in vitro. **Brain research Brain research reviews**. 2005;49:377-387.
38. Martin-Caraballo M, Greer JJ. Electrophysiological properties of rat phrenic motoneurons during perinatal development. **Journal of neurophysiology**. 1999;81:1365-1378.
39. Gao BX, Ziskind-Conhaim L. Development of ionic currents underlying changes in action potential waveforms in rat spinal motoneurons. **Journal of neurophysiology**. 1998;80:3047-3061.
40. Takazawa T, Croft GF, Amoroso MW, Studer L, Wichterle H, Macdermott AB. Maturation of spinal motor neurons derived from human embryonic stem cells. **PloS one**. 2012;7:e40154.
41. Alessandri-Haber N, Alcaraz G, Deleuze C, Jullien F, Manrique C, Couraud F, Crest M, Giraud P. Molecular determinants of emerging excitability in rat embryonic motoneurons. **The Journal of physiology**. 2002;541:25-39.
42. Rekling JC, Funk GD, Bayliss DA, Dong XW, Feldman JL. Synaptic control of motoneuronal excitability. **Physiological reviews**. 2000;80:767-852.
43. Larsson HP. What determines the kinetics of the slow afterhyperpolarization (sAHP) in neurons? **Biophysical journal**. 2013;104:281-283.
44. McCobb DP, Best PM, Beam KG. The differentiation of excitability in embryonic chick limb motoneurons. **The Journal of neuroscience : the official journal of the Society for Neuroscience**. 1990;10:2974-2984.
45. McCobb DP, Best PM, Beam KG. Development alters the expression of calcium currents in chick limb motoneurons. **Neuron**. 1989;2:1633-1643.
46. Frey D, Schneider C, Xu L, Borg J, Spooren W, Caroni P. Early and selective loss of neuromuscular synapse subtypes with low sprouting competence in motoneuron diseases. **The Journal of neuroscience : the official journal of the Society for Neuroscience**. 2000;20:2534-2542.
47. Stein RB, Parmiggiani F. Optimal motor patterns for activating mammalian muscle. **Brain research**. 1979;175:372-376.
48. Alexianu ME, Ho BK, Mohamed AH, La Bella V, Smith RG, Appel SH. The role of calcium-binding proteins in selective motoneuron vulnerability in amyotrophic lateral sclerosis. **Annals of neurology**. 1994;36:846-858.
49. von Lewinski F, Keller BU. Ca2+, mitochondria and selective motoneuron vulnerability: implications for ALS. **Trends Neurosci**. 2005;28:494-500.

50. Carriedo SG, Sensi SL, Yin HZ, Weiss JH. AMPA exposures induce mitochondrial Ca(2+) overload and ROS generation in spinal motor neurons in vitro. **The Journal of neuroscience : the official journal of the Society for Neuroscience**. 2000;20:240-250.
51. Grosskreutz J, Haastert K, Dewil M, Van Damme P, Callewaert G, Robberecht W, Dengler R, Van Den Bosch L. Role of mitochondria in kainate-induced fast Ca2+ transients in cultured spinal motor neurons. **Cell calcium**. 2007;42:59-69.
52. Bergmann F, Keller BU. Impact of mitochondrial inhibition on excitability and cytosolic Ca2+ levels in brainstem motoneurones from mouse. **The Journal of physiology**. 2004;555:45-59.
53. Heath PR, Tomkins J, Ince PG, Shaw PJ. Quantitative assessment of AMPA receptor mRNA in human spinal motor neurons isolated by laser capture microdissection. **Neuroreport**. 2002;13:1753-1757.
54. Kawahara Y, Kwak S, Sun H, Ito K, Hashida H, Aizawa H, Jeong SY, Kanazawa I. Human spinal motoneurons express low relative abundance of GluR2 mRNA: an implication for excitotoxicity in ALS. **Journal of neurochemistry**. 2003;85:680-689.
55. Rothstein JD, Martin LJ, Kuncl RW. Decreased glutamate transport by the brain and spinal cord in amyotrophic lateral sclerosis. **The New England journal of medicine**. 1992;326:1464-1468.
56. Rothstein JD, Van Kammen M, Levey AI, Martin LJ, Kuncl RW. Selective loss of glial glutamate transporter GLT-1 in amyotrophic lateral sclerosis. **Annals of neurology**. 1995;38:73-84.
57. Jiang Z, Rempel J, Li J, Sawchuk MA, Carlin KP, Brownstone RM. Development of L-type calcium channels and a nifedipine-sensitive motor activity in the postnatal mouse spinal cord. **The European journal of neuroscience**. 1999;11:3481-3487.
58. Simon M, Perrier JF, Hounsgaard J. Subcellular distribution of L-type Ca2+ channels responsible for plateau potentials in motoneurons from the lumbar spinal cord of the turtle. **The European journal of neuroscience**. 2003;18:258-266.
59. Xu W, Lipscombe D. Neuronal Ca(V)1.3alpha(1) L-type channels activate at relatively hyperpolarized membrane potentials and are incompletely inhibited by dihydropyridines. **The Journal of neuroscience : the official journal of the Society for Neuroscience**. 2001;21:5944-5951.
60. Quinlan KA, Schuster JE, Fu R, Siddique T, Heckman CJ. Altered postnatal maturation of electrical properties in spinal motoneurons in a mouse model of amyotrophic lateral sclerosis. **The Journal of physiology**. 2011;589:2245-2260.
61. Heckman CJ, Johnson M, Mottram C, Schuster J. Persistent inward currents in spinal motoneurons and their influence on human motoneuron firing patterns. **The Neuroscientist : a review journal bringing neurobiology, neurology and psychiatry**. 2008;14:264-275.
62. Li Y, Bennett DJ. Persistent sodium and calcium currents cause plateau potentials in motoneurons of chronic spinal rats. **Journal of neurophysiology**. 2003;90:857-869.
63. ElBasiouny SM, Schuster JE, Heckman CJ. Persistent inward currents in spinal motoneurons: important for normal function but potentially harmful after spinal cord injury and in amyotrophic lateral sclerosis. **Clinical neurophysiology : official journal of the International Federation of Clinical Neurophysiology**. 2010;121:1669-1679.
64. Lee RH, Heckman CJ. Essential role of a fast persistent inward current in action potential initiation and control of rhythmic firing. **Journal of neurophysiology**. 2001;85:472-475.

65. Hounsgaard J, Kiehn O. Serotonin-induced bistability of turtle motoneurones caused by a nifedipine-sensitive calcium plateau potential. **The Journal of physiology**. 1989;414:265-282.
66. Quinlan KA, Schuster JE, Fu R, Siddique T, Heckman CJ. Altered postnatal maturation of electrical properties in spinal motoneurons in a mouse model of amyotrophic lateral sclerosis. **J Physiol**. 2011;589:2245-2260.
67. Dimitriadi M, Kye MJ, Kalloo G, Yersak JM, Sahin M, Hart AC. The neuroprotective drug riluzole acts via small conductance Ca2+-activated K+ channels to ameliorate defects in spinal muscular atrophy models. **The Journal of neuroscience : the official journal of the Society for Neuroscience**. 2013;33:6557-6562.
68. Vucic S, Kiernan MC. Novel threshold tracking techniques suggest that cortical hyperexcitability is an early feature of motor neuron disease. **Brain : a journal of neurology**. 2006;129:2436-2446.
69. Eisen A, Pant B, Stewart H. Cortical excitability in amyotrophic lateral sclerosis: a clue to pathogenesis. **The Canadian journal of neurological sciences Le journal canadien des sciences neurologiques**. 1993;20:11-16.
70. Mogyoros I, Kiernan MC, Burke D, Bostock H. Strength-duration properties of sensory and motor axons in amyotrophic lateral sclerosis. **Brain : a journal of neurology**. 1998;121 ( Pt 5):851-859.
71. Kuo JJ, Schonewille M, Siddique T, Schults AN, Fu R, Bar PR, Anelli R, Heckman CJ, Kroese AB. Hyperexcitability of cultured spinal motoneurons from presymptomatic ALS mice. **Journal of neurophysiology**. 2004;91:571-575.
72. Pieri M, Albo F, Gaetti C, Spalloni A, Bengtson CP, Longone P, Cavalcanti S, Zona C. Altered excitability of motor neurons in a transgenic mouse model of familial amyotrophic lateral sclerosis. **Neuroscience letters**. 2003;351:153-156.
73. Saba L, Viscomi MT, Caioli S, Pignataro A, Bisicchia E, Pieri M, Molinari M, Ammassari-Teule M, Zona C. Altered Functionality, Morphology, and Vesicular Glutamate Transporter Expression of Cortical Motor Neurons from a Presymptomatic Mouse Model of Amyotrophic Lateral Sclerosis. **Cerebral cortex**. 2015.
74. Kanai K, Kuwabara S, Misawa S, Tamura N, Ogawara K, Nakata M, Sawai S, Hattori T, Bostock H. Altered axonal excitability properties in amyotrophic lateral sclerosis: impaired potassium channel function related to disease stage. **Brain : a journal of neurology**. 2006;129:953-962.
75. Bostock H, Sharief MK, Reid G, Murray NM. Axonal ion channel dysfunction in amyotrophic lateral sclerosis. **Brain : a journal of neurology**. 1995;118 ( Pt 1):217-225.
76. Shibuya K, Misawa S, Arai K, Nakata M, Kanai K, Yoshiyama Y, Ito K, Isose S, Noto Y, Nasu S, Sekiguchi Y, Fujimaki Y, Ohmori S, Kitamura H, Sato Y, Kuwabara S. Markedly reduced axonal potassium channel expression in human sporadic amyotrophic lateral sclerosis: an immunohistochemical study. **Experimental neurology**. 2011;232:149-153.
77. Zona C, Pieri M, Carunchio I. Voltage-dependent sodium channels in spinal cord motor neurons display rapid recovery from fast inactivation in a mouse model of amyotrophic lateral sclerosis. **Journal of neurophysiology**. 2006;96:3314-3322.
78. Thomson JA, Itskovitz-Eldor J, Shapiro SS, Waknitz MA, Swiergiel JJ, Marshall VS, Jones JM. Embryonic stem cell lines derived from human blastocysts. **Science**. 1998;282:1145-1147.

79. Wilmut I, Schnieke AE, McWhir J, Kind AJ, Campbell KH. Viable offspring derived from fetal and adult mammalian cells. **Nature**. 1997;385:810-813.
80. Cowan CA, Atienza J, Melton DA, Eggan K. Nuclear reprogramming of somatic cells after fusion with human embryonic stem cells. **Science**. 2005;309:1369-1373.
81. Tada M, Takahama Y, Abe K, Nakatsuji N, Tada T. Nuclear reprogramming of somatic cells by in vitro hybridization with ES cells. **Current biology : CB**. 2001;11:1553-1558.
82. Takahashi K, Yamanaka S. Induction of pluripotent stem cells from mouse embryonic and adult fibroblast cultures by defined factors. **Cell**. 2006;126:663-676.
83. Takahashi K, Tanabe K, Ohnuki M, Narita M, Ichisaka T, Tomoda K, Yamanaka S. Induction of pluripotent stem cells from adult human fibroblasts by defined factors. **Cell**. 2007;131:861-872.
84. Loh YH, Agarwal S, Park IH, Urbach A, Huo H, Heffner GC, Kim K, Miller JD, Ng K, Daley GQ. Generation of induced pluripotent stem cells from human blood. **Blood**. 2009;113:5476-5479.
85. Ye Z, Zhan H, Mali P, Dowey S, Williams DM, Jang YY, Dang CV, Spivak JL, Moliterno AR, Cheng L. Human-induced pluripotent stem cells from blood cells of healthy donors and patients with acquired blood disorders. **Blood**. 2009;114:5473-5480.
86. Lindner SE, Sugden B. The plasmid replicon of Epstein-Barr virus: mechanistic insights into efficient, licensed, extrachromosomal replication in human cells. **Plasmid**. 2007;58:1-12.
87. Marchetto MC, Yeo GW, Kainohana O, Marsala M, Gage FH, Muotri AR. Transcriptional signature and memory retention of human-induced pluripotent stem cells. **PloS one**. 2009;4:e7076.
88. Yu J, Hu K, Smuga-Otto K, Tian S, Stewart R, Slukvin, II, Thomson JA. Human induced pluripotent stem cells free of vector and transgene sequences. **Science**. 2009;324:797-801.
89. Chou BK, Mali P, Huang X, Ye Z, Dowey SN, Resar LM, Zou C, Zhang YA, Tong J, Cheng L. Efficient human iPS cell derivation by a non-integrating plasmid from blood cells with unique epigenetic and gene expression signatures. **Cell research**. 2011;21:518-529.
90. Dowey SN, Huang X, Chou BK, Ye Z, Cheng L. Generation of integration-free human induced pluripotent stem cells from postnatal blood mononuclear cells by plasmid vector expression. **Nature protocols**. 2012;7:2013-2021.
91. Dimos JT, Rodolfa KT, Niakan KK, Weisenthal LM, Mitsumoto H, Chung W, Croft GF, Saphier G, Leibel R, Goland R, Wichterle H, Henderson CE, Eggan K. Induced pluripotent stem cells generated from patients with ALS can be differentiated into motor neurons. **Science**. 2008;321:1218-1221.
92. Egawa N, Kitaoka S, Tsukita K, Naitoh M, Takahashi K, Yamamoto T, Adachi F, Kondo T, Okita K, Asaka I, Aoi T, Watanabe A, Yamada Y, Morizane A, Takahashi J, Ayaki T, Ito H, Yoshikawa K, Yamawaki S, Suzuki S, Watanabe D, Hioki H, Kaneko T, Makioka K, Okamoto K, Takuma H, Tamaoka A, Hasegawa K, Nonaka T, Hasegawa M, Kawata A, Yoshida M, Nakahata T, Takahashi R, Marchetto MC, Gage FH, Yamanaka S, Inoue H. Drug screening for ALS using patient-specific induced pluripotent stem cells. **Science translational medicine**. 2012;4:145ra104.
93. Bilican B, Serio A, Barmada SJ, Nishimura AL, Sullivan GJ, Carrasco M, Phatnani HP, Puddifoot CA, Story D, Fletcher J, Park IH, Friedman BA, Daley GQ, Wyllie DJ,

Hardingham GE, Wilmut I, Finkbeiner S, Maniatis T, Shaw CE, Chandran S. Mutant induced pluripotent stem cell lines recapitulate aspects of TDP-43 proteinopathies and reveal cell-specific vulnerability. **Proceedings of the National Academy of Sciences of the United States of America**. 2012;109:5803-5808.

94. Sareen D, O'Rourke JG, Meera P, Muhammad AK, Grant S, Simpkinson M, Bell S, Carmona S, Ornelas L, Sahabian A, Gendron T, Petrucelli L, Baughn M, Ravits J, Harms MB, Rigo F, Bennett CF, Otis TS, Svendsen CN, Baloh RH. Targeting RNA foci in iPSC-derived motor neurons from ALS patients with a C9ORF72 repeat expansion. **Science translational medicine**. 2013;5:208ra149.
95. Donnelly CJ, Zhang PW, Pham JT, Haeusler AR, Mistry NA, Vidensky S, Daley EL, Poth EM, Hoover B, Fines DM, Maragakis N, Tienari PJ, Petrucelli L, Traynor BJ, Wang J, Rigo F, Bennett CF, Blackshaw S, Sattler R, Rothstein JD. RNA toxicity from the ALS/FTD C9ORF72 expansion is mitigated by antisense intervention. **Neuron**. 2013;80:415-428.
96. Mitne-Neto M, Machado-Costa M, Marchetto MC, Bengtson MH, Joazeiro CA, Tsuda H, Bellen HJ, Silva HC, Oliveira AS, Lazar M, Muotri AR, Zatz M. Downregulation of VAPB expression in motor neurons derived from induced pluripotent stem cells of ALS8 patients. **Human molecular genetics**. 2011;20:3642-3652.
97. Burkhardt MF, Martinez FJ, Wright S, Ramos C, Volfson D, Mason M, Garnes J, Dang V, Lievers J, Shoukat-Mumtaz U, Martinez R, Gai H, Blake R, Vaisberg E, Grskovic M, Johnson C, Irion S, Bright J, Cooper B, Nguyen L, Griswold-Prenner I, Javaherian A. A cellular model for sporadic ALS using patient-derived induced pluripotent stem cells. **Molecular and cellular neurosciences**. 2013;56:355-364.
98. Wainger BJ, Kiskinis E, Mellin C, Wiskow O, Han SS, Sandoe J, Perez NP, Williams LA, Lee S, Boulting G, Berry JD, Brown RH, Jr., Cudkowicz ME, Bean BP, Eggan K, Woolf CJ. Intrinsic membrane hyperexcitability of amyotrophic lateral sclerosis patient-derived motor neurons. **Cell reports**. 2014;7:1-11.
99. Hideyama T, Yamashita T, Aizawa H, Tsuji S, Kakita A, Takahashi H, Kwak S. Profound downregulation of the RNA editing enzyme ADAR2 in ALS spinal motor neurons. **Neurobiology of disease**. 2012;45:1121-1128.
100. Zhang J, Khvorostov I, Hong JS, Oktay Y, Vergnes L, Nuebel E, Wahjudi PN, Setoguchi K, Wang G, Do A, Jung HJ, McCaffery JM, Kurland IJ, Reue K, Lee WN, Koehler CM, Teitell MA. UCP2 regulates energy metabolism and differentiation potential of human pluripotent stem cells. **Embo J**. 2011;30:4860-4873.
101. Xu X, Duan S, Yi F, Ocampo A, Liu GH, Izpisua Belmonte JC. Mitochondrial regulation in pluripotent stem cells. **Cell Metab**. 2013;18:325-332.
102. Zhang J, Nuebel E, Daley GQ, Koehler CM, Teitell MA. Metabolic regulation in pluripotent stem cells during reprogramming and self-renewal. **Cell stem cell**. 2012;11:589-595.
103. Folmes CD, Dzeja PP, Nelson TJ, Terzic A. Metabolic plasticity in stem cell homeostasis and differentiation. **Cell stem cell**. 2012;11:596-606.
104. Prigione A, Fauler B, Lurz R, Lehrach H, Adjaye J. The senescence-related mitochondrial/oxidative stress pathway is repressed in human induced pluripotent stem cells. **Stem cells**. 2010;28:721-733.
105. St John JC, Amaral A, Bowles E, Oliveira JF, Lloyd R, Freitas M, Gray HL, Navara CS, Oliveira G, Schatten GP, Spikings E, Ramalho-Santos J. The analysis of mitochondria

and mitochondrial DNA in human embryonic stem cells. **Methods in molecular biology**. 2006;331:347-374.
106. Facucho-Oliveira JM, Alderson J, Spikings EC, Egginton S, St John JC. Mitochondrial DNA replication during differentiation of murine embryonic stem cells. **J Cell Sci**. 2007;120:4025-4034.
107. Birket MJ, Orr AL, Gerencser AA, Madden DT, Vitelli C, Swistowski A, Brand MD, Zeng X. A reduction in ATP demand and mitochondrial activity with neural differentiation of human embryonic stem cells. **J Cell Sci**. 2011;124:348-358.
108. Cho YM, Kwon S, Pak YK, Seol HW, Choi YM, Park do J, Park KS, Lee HK. Dynamic changes in mitochondrial biogenesis and antioxidant enzymes during the spontaneous differentiation of human embryonic stem cells. **Biochem Biophys Res Commun**. 2006;348:1472-1478.
109. Saretzki G, Walter T, Atkinson S, Passos JF, Bareth B, Keith WN, Stewart R, Hoare S, Stojkovic M, Armstrong L, von Zglinicki T, Lako M. Downregulation of multiple stress defense mechanisms during differentiation of human embryonic stem cells. **Stem Cells**. 2008;26:455-464.
110. Zhang J, Khvorostov I, Hong JS, Oktay Y, Vergnes L, Nuebel E, Wahjudi PN, Setoguchi K, Wang G, Do A, Jung HJ, McCaffery JM, Kurland IJ, Reue K, Lee WN, Koehler CM, Teitell MA. UCP2 regulates energy metabolism and differentiation potential of human pluripotent stem cells. **The EMBO journal**. 2011;30:4860-4873.
111. Vozza A, Parisi G, De Leonardis F, Lasorsa FM, Castegna A, Amorese D, Marmo R, Calcagnile VM, Palmieri L, Ricquier D, Paradies E, Scarcia P, Palmieri F, Bouillaud F, Fiermonte G. UCP2 transports C4 metabolites out of mitochondria, regulating glucose and glutamine oxidation. **Proceedings of the National Academy of Sciences of the United States of America**. 2014;111:960-965.
112. Rupprecht A, Sittner D, Smorodchenko A, Hilse KE, Goyn J, Moldzio R, Seiler AE, Brauer AU, Pohl EE. Uncoupling protein 2 and 4 expression pattern during stem cell differentiation provides new insight into their putative function. **PloS one**. 2014;9:e88474.
113. Prigione A, Rohwer N, Hoffmann S, Mlody B, Drews K, Bukowiecki R, Blumlein K, Wanker EE, Ralser M, Cramer T, Adjaye J. HIF1alpha modulates cell fate reprogramming through early glycolytic shift and upregulation of PDK1-3 and PKM2. **Stem cells**. 2014;32:364-376.
114. Goda F, O'Hara JA, Liu KJ, Rhodes ES, Dunn JF, Swartz HM. Comparisons of measurements of pO2 in tissue in vivo by EPR oximetry and microelectrodes. **Advances in experimental medicine and biology**. 1997;411:543-549.
115. Clarke L, van der Kooy D. Low oxygen enhances primitive and definitive neural stem cell colony formation by inhibiting distinct cell death pathways. **Stem Cells**. 2009;27:1879-1886.
116. Studer L, Csete M, Lee SH, Kabbani N, Walikonis J, Wold B, McKay R. Enhanced proliferation, survival, and dopaminergic differentiation of CNS precursors in lowered oxygen. **J Neurosci**. 2000;20:7377-7383.
117. Stacpoole SR, Bilican B, Webber DJ, Luzhynskaya A, He XL, Compston A, Karadottir R, Franklin RJ, Chandran S. Efficient derivation of NPCs, spinal motor neurons and midbrain dopaminergic neurons from hESCs at 3% oxygen. **Nat Protoc**. 2011;6:1229-1240.

118. Horie N, So K, Moriya T, Kitagawa N, Tsutsumi K, Nagata I, Shinohara K. Effects of oxygen concentration on the proliferation and differentiation of mouse neural stem cells in vitro. **Cellular and molecular neurobiology**. 2008;28:833-845.
119. Yan Y, Shin S, Jha BS, Liu Q, Sheng J, Li F, Zhan M, Davis J, Bharti K, Zeng X, Rao M, Malik N, Vemuri MC. Efficient and rapid derivation of primitive neural stem cells and generation of brain subtype neurons from human pluripotent stem cells. **Stem cells translational medicine**. 2013;2:862-870.
120. Li XJ, Du ZW, Zarnowska ED, Pankratz M, Hansen LO, Pearce RA, Zhang SC. Specification of motoneurons from human embryonic stem cells. **Nat Biotechnol**. 2005;23:215-221.
121. Singh Roy N, Nakano T, Xuing L, Kang J, Nedergaard M, Goldman SA. Enhancer-specified GFP-based FACS purification of human spinal motor neurons from embryonic stem cells. **Exp Neurol**. 2005;196:224-234.
122. Lee H, Shamy GA, Elkabetz Y, Schofield CM, Harrsion NL, Panagiotakos G, Socci ND, Tabar V, Studer L. Directed differentiation and transplantation of human embryonic stem cell-derived motoneurons. **Stem Cells**. 2007;25:1931-1939.
123. Zeng H, Guo M, Martins-Taylor K, Wang X, Zhang Z, Park JW, Zhan S, Kronenberg MS, Lichtler A, Liu HX, Chen FP, Yue L, Li XJ, Xu RH. Specification of region-specific neurons including forebrain glutamatergic neurons from human induced pluripotent stem cells. **PLoS One**. 2010;5:e11853.
124. Marchetto MC, Muotri AR, Mu Y, Smith AM, Cezar GG, Gage FH. Non-cell-autonomous effect of human SOD1 G37R astrocytes on motor neurons derived from human embryonic stem cells. **Cell stem cell**. 2008;3:649-657.
125. Amoroso MW, Croft GF, Williams DJ, O'Keeffe S, Carrasco MA, Davis AR, Roybon L, Oakley DH, Maniatis T, Henderson CE, Wichterle H. Accelerated high-yield generation of limb-innervating motor neurons from human stem cells. **J Neurosci**. 2013;33:574-586.
126. Wang ZB, Zhang X, Li XJ. Recapitulation of spinal motor neuron-specific disease phenotypes in a human cell model of spinal muscular atrophy. **Cell Res**. 2013;23:378-393.
127. Li XJ, Hu BY, Jones SA, Zhang YS, Lavaute T, Du ZW, Zhang SC. Directed differentiation of ventral spinal progenitors and motor neurons from human embryonic stem cells by small molecules. **Stem cells**. 2008;26:886-893.
128. Amoroso MW, Croft GF, Williams DJ, O'Keeffe S, Carrasco MA, Davis AR, Roybon L, Oakley DH, Maniatis T, Henderson CE, Wichterle H. Accelerated high-yield generation of limb-innervating motor neurons from human stem cells. **The Journal of neuroscience : the official journal of the Society for Neuroscience**. 2013;33:574-586.
129. Keeney PM, Quigley CK, Dunham LD, Papageorge CM, Iyer S, Thomas RR, Schwarz KM, Trimmer PA, Khan SM, Portell FR, Bergquist KE, Bennett JP, Jr. Mitochondrial gene therapy augments mitochondrial physiology in a Parkinson's disease cell model. **Human gene therapy**. 2009;20:897-907.
130. Cronin-Furman EN, Borland MK, Bergquist KE, Bennett JP, Jr., Trimmer PA. Mitochondrial quality, dynamics and functional capacity in Parkinson's disease cybrid cell lines selected for Lewy body expression. **Molecular neurodegeneration**. 2013;8:6.
131. Chen H, Qian K, Du Z, Cao J, Petersen A, Liu H, Blackbourn LWt, Huang CL, Errigo A, Yin Y, Lu J, Ayala M, Zhang SC. Modeling ALS with iPSCs reveals that mutant SOD1 misregulates neurofilament balance in motor neurons. **Cell stem cell**. 2014;14:796-809.

132. Kiskinis E, Sandoe J, Williams LA, Boulting GL, Moccia R, Wainger BJ, Han S, Peng T, Thams S, Mikkilineni S, Mellin C, Merkle FT, Davis-Dusenbery BN, Ziller M, Oakley D, Ichida J, Di Costanzo S, Atwater N, Maeder ML, Goodwin MJ, Nemesh J, Handsaker RE, Paull D, Noggle S, McCarroll SA, Joung JK, Woolf CJ, Brown RH, Eggan K. Pathways disrupted in human ALS motor neurons identified through genetic correction of mutant SOD1. **Cell stem cell**. 2014;14:781-795.
133. Chestkov IV, Vasilieva EA, Illarioshkin SN, Lagarkova MA, Kiselev SL. Patient-Specific Induced Pluripotent Stem Cells for SOD1-Associated Amyotrophic Lateral Sclerosis Pathogenesis Studies. **Acta naturae**. 2014;6:54-60.
134. Zhang Z, Almeida S, Lu Y, Nishimura AL, Peng L, Sun D, Wu B, Karydas AM, Tartaglia MC, Fong JC, Miller BL, Farese RV, Jr., Moore MJ, Shaw CE, Gao FB. Downregulation of microRNA-9 in iPSC-derived neurons of FTD/ALS patients with TDP-43 mutations. **PloS one**. 2013;8:e76055.
135. Serwold T, Hochedlinger K, Inlay MA, Jaenisch R, Weissman IL. Early TCR expression and aberrant T cell development in mice with endogenous prerearranged T cell receptor genes. **Journal of immunology**. 2007;179:928-938.
136. Michalczyk K, Ziman M. Nestin structure and predicted function in cellular cytoskeletal organisation. **Histology and histopathology**. 2005;20:665-671.
137. Zhang J, Nuebel E, Wisidagama DR, Setoguchi K, Hong JS, Van Horn CM, Imam SS, Vergnes L, Malone CS, Koehler CM, Teitell MA. Measuring energy metabolism in cultured cells, including human pluripotent stem cells and differentiated cells. **Nature protocols**. 2012;7:1068-1085.
138. Boulting GL, Kiskinis E, Croft GF, Amoroso MW, Oakley DH, Wainger BJ, Williams DJ, Kahler DJ, Yamaki M, Davidow L, Rodolfa CT, Dimos JT, Mikkilineni S, MacDermott AB, Woolf CJ, Henderson CE, Wichterle H, Eggan K. A functionally characterized test set of human induced pluripotent stem cells. **Nature biotechnology**. 2011;29:279-286.
139. Chambers SM, Fasano CA, Papapetrou EP, Tomishima M, Sadelain M, Studer L. Highly efficient neural conversion of human ES and iPS cells by dual inhibition of SMAD signaling. **Nature biotechnology**. 2009;27:275-280.
140. Knight E, Przyborski S. Advances in 3D cell culture technologies enabling tissue-like structures to be created in vitro. **Journal of anatomy**. 2014.
141. Lu B, Pang PT, Woo NH. The yin and yang of neurotrophin action. **Nature reviews Neuroscience**. 2005;6:603-614.
142. Cai J, Hua F, Yuan L, Tang W, Lu J, Yu S, Wang X, Hu Y. Potential therapeutic effects of neurotrophins for acute and chronic neurological diseases. **BioMed research international**. 2014;2014:601084.

# LAURA O'BRIEN
obrienl@vcu.edu


## EDUCATION

Bachelor of Science Psychology, Biology minor, Kansas State University 2010
PhD in Physiology and Biophysics, Virginia Commonwealth University, May 2015

## PREVIOUS RESEARCH EXPERIENCE:

**Ph.D. Candidate** (July 2011 – present)
Virginia Commonwealth University
Department of Physiology and Biophysics
Advisor: James P. Bennett, Jr., MD, Ph.D.

**Research Assistant** (January 2010 – June 2011)
Kansas State University College of Veterinary Medicine
Diagnostic Medicine/Pathobiology
Advisor: Raymond R. R. Rowland, Ph.D.

**Research Assistant/Animal Care Technician** (January 2007 – December 2009)
Kansas State University
Department of Psychology
Advisor: Matthew Palmatier, Ph.D.

## MEMBERSHIPS IN PROFESSIONAL SOCIETIES:

Central Virginia Chapter of the Society for Neuroscience
American Association for the Advancement of Science
Society for Neuroscience

## SPECIAL TRAINING:

Clinical and Translational Research Course for Ph.D. Students at the NIH Clinical Center
July 8-19 2013 at the NIH Bethesda, MD campus

## HONORS AND AWARDS:

Best Presentation, 17$^{th}$ Annual Graduate Student Research Symposium & Exhibit, 2014
Member, Phi Kappa Phi honor society, 2013
Outstanding Service Project of the Year for Girl Scout Science Day, 2013

Kansas State University EJ Phares Prize for Outstanding Undergraduate Research, 2009
Kansas State University Doreen Shanteau Undergraduate Research Fellowship, 2009

## LEADERSHIP POSITIONS

Graduate Student Association, Virginia Commonwealth University
- Representative Council 2013-2014
- Executive Committee, Events/philanthropy chair 2014-2015

Women in Science, Virginia Commonwealth University
- President 2013-2014
- Vice President of Community Outreach 2012-2013

22nd Annual WISDM Leadership Conference Planning Committee 2014
Vice President of Psi Chi 2009-2010
Undergraduate Teaching Practicum 2008, 2009

## PUBLICATIONS

1. **O'Brien LC**, Keeney PM, Bennett JP, Jr. Differentiation of Human Neural Stem Cells into Motor Neurons Stimulates Mitochondrial Biogenesis and Decreases Glycolytic Flux. **Stem cells and development**. 2015.
2. **O'Brien LC**, Mezzaroma E, Van Tassell BW, Marchetti C, Carbone S, Abbate A, Toldo S. Interleukin-18 as a therapeutic target in acute myocardial infarction and heart failure. **Molecular medicine**. 2014;20:221-229.
3. Toldo S, Mezzaroma E, **O'Brien L**, Marchetti C, Seropian IM, Voelkel NF, Van Tassell BW, Dinarello CA, Abbate A. Interleukin-18 mediates interleukin-1-induced cardiac dysfunction. **American journal of physiology Heart and circulatory physiology**. 2014;306:H1025-1031.
4. Palmatier MI, Lantz JE, **O'Brien LC**, Metz SP. Effects of nicotine on olfactogustatory incentives: preference, palatability, and operant choice tests. **Nicotine & tobacco research : official journal of the Society for Research on Nicotine and Tobacco**. 2013;15:1545-1554.
5. Palmatier MI, **O'Brien LC**, Hall MJ. The role of conditioning history and reinforcer strength in the reinforcement enhancing effects of nicotine in rats. **Psychopharmacology**. 2012;219:1119-1131.

## SCIENTIFIC MEETING ABSTRACTS/PRESENTATIONS:

**O'Brien LC** and J.P. Bennett, Jr. 2014. Differentiation of human neural stem cells to a motor neuron phenotype stimulates mitochondrial biogenesis. Abstract for poster presentation. 44th annual meeting of the Society for Neuroscience.

Brohawn DG, **O'Brien L**, Gravanis A, Bennett, JP, Jr. 2014. Effects of a microneurotrophin on gene expression in an *in vitro* human motor neuron model. Abstract for poster presentation. 44th annual meeting of the Society for Neuroscience.

**O'Brien LC** and Bennett JP, Jr. 2014. Differentiation of human neural stem cells to a motor neuron phenotype increases mitochondrial biogenesis. 42nd annual John C. Forbes Research Colloquium, Virginia Commonwealth University.

**O'Brien L.** 2014. Mitochondrial changes during the differentiation of human cells into motor neurons. Abstract for poster presentation. 17th annual graduate student research symposium & Exhibit, Virginia Commonwealth University.

**O'Brien L** and Bennett JP, Jr. 2014. Mitochondrial biogenesis gene expression during the differentiation of human neural stem cells into motor neurons. Abstract for poster presentation. Annual Symposium of the Central Virginia Chapter of the Society for Neuroscience.

**O'Brien LC** and Bennett JP, Jr. 2014. Changes in mitochondria as cells mature from human neural stem cells to mature motor neurons. Abstract for poster presentation. Keystone symposia on molecular and cellular biology meeting on mitochondrial dynamics and physiology.

Marchetti C, Mezzaroma E, **O'Brien LC**, Tancrida N, Van Tassell BW, Voelkel NF, Abbate A, and Toldo S. 2013. Dual role of the P2X7 receptor in the cardiomyocyte: induction of autophagy and formation of the NLRP3 inflammasome. Abstract for oral presentation. Annual meeting of the American Hearth Association.

Levesque S, Wagner A, **O'Brien LC**, McGraw C, Block ML. 2011. Paraquat primes microglial activation and dopaminergic neurotoxicity through NOX2 & NF-κB p50. Abstract for poster presentation. 51st annual meeting of society of toxicology.

**O'Brien LC**, Rowland RR. 2011. Nuclear export of non-structural protein 1 and nucleocapsid protein of porcine reproductive and respiratory syndrome virus (PRRSV). Abstract for oral presentation. American Society for Microbiology-Missouri Valley Branch Meeting.

**O'Brien LC,** Rowland RR. 2011. Nuclear export of structural and nonstructural proteins of porcine reproductive and respiratory virus (PRRSV). Abstract for oral presentation. Phi Zeta Research Day.

**Dare LC**, Palmatier MI. 2009. Nicotine increases the motivation to obtain sucrose reinforcement on a progressive ratio schedule. Abstract for poster presentation. 25th Annual Undergraduate Research Convocation.

Lantz JE, **Dare LC**, Deehan J, Joseph C, Kiefer SW, Palmatier MI. 2009. The effect of nicotine on taste reactivity to sucrose and ethanol. Abstract for poster presentation. 39th Annual Meeting of the Society for Neuroscience.

**Dare LC**, Hall MJ, Bluvan D, Deehan J, Palmatier MI. 2008. Nicotine enhances the motivation to obtain sucrose on a PR schedule but decreases sucrose-intake in free-

access tests. Abstract for poster presentation. 38th Annual Meeting of the Society for Neuroscience.